Investigating Sire Fertility: The Relationship between Spermatozoa Characteristics and Early Embryonic Development

---

A Thesis

Presented to

The Faculty of the Graduate School

University of Missouri- Columbia

In Partial Fulfillment

Of the Requirements for the Degree

Master of Science

By

Lindsey Cole Fallon

Dr. M. Sofia Ortega- Thesis Supervisor

December 2022

The following, appointed by the Dean of the Graduate School, have examined the thesis entitled:

Investigating Sire Fertility: The Relationship between Spermatozoa Characteristics and Early Embryonic Development

Presented by **Lindsey Cole Fallon**
A candidate for the degree of Master of Science
And hereby certify that in our opinion it is worthy of acceptance

Dr. M. Sofia Ortega

Dr. Peter Sutovsky

Dr. Yuksel Agca

Dr. Christopher Tubbs

Acknowledgements

There are many people whom I would like to thank for their support and help throughout my master's program. I would first like to thank my advisor, Dr. Sofia Ortega, for providing me with the resources I needed to complete my research, assisting me with troubleshooting protocols, encouraging me to share my research at conferences, and allowing me the chance to pursue opportunities during my program which have positioned me to enter my career following graduation. I would also like to thank the Ortega lab members, past and present, for all their help during my program: Katy, Kelsey, Jessica, Ethel, and Chasi. Katy, thank you for always answering my questions about embryo culture, helping me collect oocytes for my projects, teaching me how to ultrasound cows, and for the wonderful friendship we've developed over the past two years. Kelsey, thank you for teaching me how to perform *in vitro* fertilization when I first arrived in the lab, assisting me with my first experiment, and for your continued friendship even after you graduated from the lab. Jessica, thank you for teaching me how to select good quality oocytes and how to perform embryo flushes in cows. Ethel and Chasi, thank you both for allowing me the opportunity to guide and teach you when you arrived in the lab. I have truly enjoyed working alongside my lab mates over the past two years.

I would also like to thank Dr. Peter Sutovsky and the entire Sutovsky lab for their support and collaboration during my projects. Dr. Sutovsky, thank you for encouraging me to work in your lab, always answering any questions I've had, and offering new ideas for exploration in my project. Lauren and Edgar, thank you for performing and teaching

me about the morphological analyses of spermatozoa for my project, helping me with the staining and flow cytometry of the fixed sperm samples, discussing the interpretation of our results, and the friendship we've developed. Michal, thank you for taking so much time to teach me how to properly operate the flow cytometer, helping me with the staining and flow cytometry of the live sperm samples, and helping me set up all my analysis templates for these experiments. Miriam, Alexis, and Mayra, thank you all as well, for your support during my time working in the Sutovsky lab.

Dr. Yuksel Agca, thank you for serving on my thesis committee and for asking intriguing questions during my committee meeting. Dr. Chris Tubbs, thank you for providing me with mentorship over the past few years, allowing me an opportunity to be a research fellow in your lab during my program, and offering me the incredible opportunity to return and work in your lab. I would also like to thank both Dr. Mike Smith and Dr. Trista Strauch for their support and guidance when applying to this graduate program—I may not have pursued this degree if it wasn't for your encouragement.

Lastly, I would like to thank my family, without whom, I never would have made it this far. To my grandma and grandpa, thank you for your unending love, support, guidance, and advice over all the years of my life. To my brother, Dalton, thank you for continuing to be one of my best friends, and the person I can always call to talk to at the end of a long day. To my mom, thank you for never hesitating to encourage me to chase my dreams, and believing in my ability to do so, no matter the odds. I would not be the person I am today if it wasn't for all the love that you've given and the important lessons that you've taught me through the years. Finally, to my husband, Bobby, I could never

thank you enough for the ways you have supported me during this program, and I wouldn't have made it here without you. I am eternally grateful to have shared all the highs and lows of the past two years with such a wonderful partner that I was always able to depend on.

Table of Contents

Abbreviations

GRP78	78-kDa Glucose-Regulated Protein
APC	Anaphase Promoting Complex
cAMP	Cyclic Adenosine Monophosphate
Ca^{2+}	Calcium
CASA	Computer Assisted Sperm Analysis
CDK1	Cyclin Dependent Kinase 1
CDX2	Caudal Type Homeobox 2
CR	Conception Rate
CRES	Cystatin-Related Epididymal Spermatogenic
CSF	Cytostatic Factor
DAG	Diacylglycerol
ER	Endoplasmic Reticulum
ERO1	Endoplasmic Reticulum Oxidoreductin-1
H_2O_2	Hydrogen Peroxide
HPI	Hours Post Insemination
IAM	Inner Acrosomal Membrane
ICM	Inner Cell Mass

IP_3	Inositol 1,4,5- Trisphosphate
IVF	*in vitro* Fertilization
KO	Knock Out
MFI	Mean Fluorescent Intensity
MPF	Maturation Promoting Factor
MTOC	Microtubule Organizing Center
NF-κB	Nuclear Factor κB
O_2	Oxygen
OAM	Outer Acrosomal Membrane
OH	Hydroxyl
PAWP	Post-acrosomal Sheath WW Domain-binding Protein
PDI	Protein Disulfide Isomerase
PI3K	Phosphatidylinositol 3-Kinase
PIP_2	Phosphatidylinositol 4,5 Bisphosphate
PKA	Protein Kinase A
PLC	Phospholipase-C
PLCζ/PLCZ1	Phospholipase-C Zeta
P-YAP	Phosphorylated YAP

RO_2	Peroxyl
ROS	Reactive Oxygen Species
REDOX	Reduction-Oxidation Reaction
SAS	Statistical Analysis Software
SCR	Sire Conception Rate
SEM	Standard Error Mean
SOAF	Sperm-borne Oocyte Activating Factor
TE	Trophectoderm
UCHL1	Ubiquitin C-terminal Hydrolase-L1
UPR	Unfolded Protein Response
UPS	Ubiquitin Proteasome System
WT	Wild Type
YAP	Yes-associated Protein 1
ZP	Zona Pellucida
ZPA	Zona Pellucida Protein A
ZPB	Zona Pellucida Protein B
ZPC	Zona Pellucida Protein C

List of Figures

Abstract

Early embryonic mortality in cattle occurs between days 1-27 of gestation and is one of the primary contributors to economic failure in the dairy industry. Specifically, by day 7 of gestation, up to 50% of all embryo mortality will have already occurred. Many critical events that determine an embryo's viability occur within the first week of development. Interestingly, it is during this time that the sire exhibits its greatest effects on pregnancy success. Commercial dairy sires differ in their ability to produce viable blastocysts, yet our understanding of the malfunction of cellular mechanisms regulated by sire during early embryo development is still lacking. This study aimed to elucidate novel biomarkers of fertility status in spermatozoa and how those differences impact mechanisms in a subsequent embryo, with a focus on cellular stress.

The elucidation of which spermatozoa characteristics impact early embryonic development has the potential to reduce the use of subfertile bulls and the incidence of early embryo mortality in the dairy cattle industry. Using modern techniques such as flow cytometry, thousands of sperm cells per sample can be accurately analyzed for a feature of interest in just minutes, which significantly increases the sample size used and decreases variability that is seen in manual, subjective evaluation under a microscope.

In this study, up to four high performing sires and four low performing sires with varying SCR values were selected for experiments based on previous classification as having high or low capacity to produce embryos *in vitro*. Fertilization, cleavage, and blastocyst rates were all recorded for embryos produced by either high or low performing sires. Next, cellular stress mechanisms in early embryos were investigated—autophagic activity and reactive oxygen species (ROS) production were measured at multiple stages

of embryo development (2-6 cell, 8-16 cell, morula, and blastocyst) in embryos produced by high or low performing sires under normal culture conditions, via fluorescent microscopy. Autophagy and ROS production were also measured in 2-6 cell embryos under induced stress conditions in the form of a heat shock. Additionally, DNA damage and lipid oxidation were assessed in 2-6 cell embryos via fluorescent microscopy.

Embryos produced by high performing sires had significantly higher cleavage and blastocyst rates compared to embryos produced by low performing sires, yet there were no differences in fertilization rates. Embryos at the 2-6 cell stage of development produced by low performing sires exhibited an increase in both ROS production and autophagic activity compared to embryos produced by high performing sires—indicating that these embryos begin development under increased cellular stress. The 2-6 cell embryos produced by low performing sires, that were exposed to a heat shock, continued to exhibit increased ROS production. There was no difference observed in the DNA damage or lipid oxidation of 2-6 cell embryos.

Next, biomarkers of sire fertility status were investigated in the spermatozoa. DNA damage was evaluated in spermatozoa both prior to gradient purification and following. Additionally, morphological assessments were performed both prior to, and following gradient purification, utilizing immunocytochemistry and epifluorescent microscopy to visualize the sperm head acrosome and nucleus, and the tail midpiece and principal piece. Finally, image-based flow cytometry was performed to quantify the presence of defective aggregated proteins that were initially identified in the spermatozoa with altered morphology, capacitation status, and membrane integrity.

In samples prior to gradient purification, or pre-gradient samples, there was an increased incidence of DNA damage in the low performing sires. Alternatively, in samples following gradient purification, or post-gradient samples, the high performing sires had increased DNA damage. Pre-gradient samples from low performing sires had increased aggregated protein content, termed aggresomes, located in the head of spermatozoa compared to high performing sires. Yet, high performing sires had increased tail defects. Using image-based flow cytometry, there were no differences found in aggresome defects of pre-gradient samples from high and low performing sires. Although, in post-gradient samples, spermatozoa from low performing sires had an increased incidence of aggresomes located in the head compared to high performing sires. Finally, post-gradient samples from low performing sires had a greater percentage of spermatozoa that were undergoing premature capacitation and had accrued membrane damage.

Currently, we have demonstrated that sire variability can impact cellular stress mechanisms and developmental competence to the blastocyst stage in early embryos, independently of SCR. Embryos at the 2-6 cell stage of development, produced by low performing sires, exhibit increased cellular stress in the form of ROS production and autophagic activity, and go on to have decreased developmental rates compared to embryos produced by high performing sires. Spermatozoa from low performing sires that have undergone gradient purification have increased aggresome defects in their heads. This indicates that the aggresomes may be incorporated into the fertilized oocyte—overwhelming protein degradation machinery in the zygote, such as autophagic machinery, leading to higher levels of cellular stress.

Chapter 1: Review of the Literature

Introduction

Pregnancy loss

Currently, it is known that pregnancy loss is the leading cause of economic failure in the dairy cattle industry (Cerri et al., 2009; Diskin & Morris, 2008; Maurer & Chenault, 1983; Wiltbank et al., 2016). Pregnancy loss can be classified under two predominant categories: early pregnancy loss which occurs between days 1-27 and late pregnancy loss which occurs from day 28 throughout gestation (Wiltbank et al., 2016). As gestation continues, the probability of embryo or fetal mortality decreases. The early pregnancy loss period is typically further divided into loss occurring during days 1-7 and days 8-27 of development. By day 7, up to 50% of all embryo mortality will have already occurred, and between days 8-27, up to 36% of embryo mortality may occur (Wiltbank et al., 2016).

It is evident that completing the first week of embryo development is a critical milestone for survival and viability. During this time, the embryo will undergo rapid developmental changes that will determine its fate in subsequent gestation. Events such as the first cellular divisions—cleavage, clearance of paternal mitochondria, embryonic genome activation, cell polarization and compaction, and cell lineage specifications are all crucial steps for embryo survival (Graf et al., 2014; Memili & First, 1999; van Soom et al., 1997). If an embryo is unable to complete any of these steps in a timely manner, it will arrest.

Sire influence on early embryonic development

There is evidence that the sire exhibits its greatest impact on pregnancy success during the events of fertilization, early embryo development, and conceptus elongation (Ortega et al., 2018). Remarkably, the spermatozoon begins regulating the fate of the future embryo immediately following penetration of an oocyte. By releasing its sperm-borne oocyte activating factor (SOAF), the spermatozoon initiates oocyte activation, including anti-polyspermy defense, release from cell cycle block/metaphase II arrest and the completion of meiosis II (Campbell et al., 2000; Nomikos et al., 2013; Sutovsky, 2018). This is followed by decondensation of the paternal chromatin and the contribution of the sperm-derived centriole—both of which are critical for the first cleavage division (Avidor-Reiss et al., 2020; Senger, 2003).

Uniparental models used to study embryo development in mice have elucidated the impact of genomic imprinting from each parental genome. It has been demonstrated that gynogenetic, or parthenogenic, embryos containing only the maternal genome develop fully formed embryos but lack extraembryonic membranes, and therefore lack placental functionality. In contrast, androgenetic embryos containing only the paternal genome exhibit severely retarded embryo development but fully functional extraembryonic membranes (Miyoshi et al., 2006). These data show the importance of male-specific contributions to embryonic development and pregnancy success.

Sire Fertility

Sire fertility measurements

The assessment of semen quality is pertinent to successful reproduction in the dairy cattle industry. Currently, semen evaluations include sperm conventional light microscopic protocols to assess the concentration, motility, and morphology of

spermatozoa. Although, no one single bioassay can correctly classify sire fertility, a combination of multiple evaluations provides some correlation to a sire's ability to successfully fertilize an oocyte and lead to a viable pregnancy (Attia et al., 2016; Harstine et al., 2018). In recent years, the use of techniques such as computer assisted sperm analysis (CASA) and biomarker-driven flow cytometry have allowed for more accurate evaluation of semen quality (Harstine et al., 2018).

In dairy cattle, sire fertility is expressed as sire conception rate (SCR)—which is defined as the probability that a given unit of semen from a specific bull will result in a viable pregnancy compared to an average bull (Norman et al., 2011). A positive value indicates increased fertility, and a negative value indicates decreased fertility. SCR is determined by confirmed pregnancies at day 70-75 post insemination—the model takes into account fixed effects of herd, year, state, month, registry status, parity, service number, daughters' milk yield, male and female ages, and breeding intervals. As well as random effects of mating year, service sire, dam, and inbreeding coefficients of the sire and the potential subsequent offspring (Kuhn et al., 2008). Although the model to calculate SCR includes many variables, it does lack the ability to incorporate important factors such as environmental stressors, female health, human error and more. Additionally, SCR cannot be established until after 300 services have occurred within a four year period (Norman et al., 2011).

Therefore, although SCR can be beneficial, relying on it alone to indicate fertility, results in three primary issues—the first being that SCR leaves room for variation from unidentified sources, as it is not in itself a direct measure of sire fertility. The second being that it is assigned after a bull has already been commercially used in the industry,

and the third being that the period prior to day 75 of gestation when the embryo or fetus undergoes mortality remains unknown (Ortega et al., 2018).

Spermatozoa defects

Morphological defects of spermatozoa are a primary cause of infertility or subfertility in males (Barth, A.D. & Oko, R.J., 1989; Gatimel et al., 2017). Defects may occur in any part of the sperm cell but are most broadly divided into head-related defects and tail-related defects and further classified into a variety of categories. One traditional system of classification is based on the origin of the defect. Defects that arise during spermatogenesis and spermiogenesis are termed primary defects, and those that arise following release from the Sertoli cells of the seminiferous tubule are termed secondary defects (Chenoweth, 2005).

Another system of classification is based on a defect's presumed impact on fertility status—minor and major defects. For an abnormality to be considered a major defect, it would also be primary, consistently occur in 10-15% of the sperm population, be associated with male infertility, and may be heritable (Chenoweth, 2005). Examples of minor defects are narrow or small head, distal cytoplasmic droplet, bent tail, and terminally coiled tail. Examples of major defects are knobbed acrosome, decapitated sperm heads, small abnormal heads, midpiece reflex, proximal cytoplasmic droplet, and strongly coiled tails ("Dag" defect) (Barth, A.D. & Oko, R.J., 1989; Chenoweth, 2005).

The third widely used system of classification is based on if the defect's impact on fertility can be alleviated by increasing the number of sperm cells present. Defects related to spermatozoa failure to reach the site of fertilization, that are thought to be alleviated by increasing sperm cell concentration are termed compensable (Chenoweth,

2005; Saacke, 2008). These defects are typically located in sperm tails. Defects related to a spermatozoon's inability to successfully fertilize or contribute to subsequent embryo development once the oocyte is reached, that cannot be alleviated by increasing sperm cell concentrations are termed non-compensable (Chenoweth, 2005; Saacke, 2008). Examples of non-compensable defects are deformed acrosome and nuclear damage, and they commonly result in embryo mortality prior to the maternal recognition of pregnancy (Saacke, 2008).

Events of Fertilization

Deposition and capacitation

Prior to successful fertilization *in vivo*, bovine spermatozoa must traverse the female reproductive tract, undergo a series of structural and biochemical changes, and reach the site of fertilization. During natural mating in cattle, semen is deposited into the vagina. Following deposition, sperm cells must swim along the cervical folds to pass the cervix and reach the uterus (Senger, 2003). It is during this time that the biochemical changes, referred to as capacitation, begin. The primed spermatozoa enter the oviduct and bind to the epithelium near the ampullary-isthmic junction, which acts as a sperm reservoir (Senger, 2003). It is not until the spermatozoa detach from the reservoir site that capacitation is completed. Capacitation is the final stage of sperm maturation. This is a critical pre-requisite for a spermatozoon to gain the ability to bind with the oocyte's zona pellucida and subsequently fuse with the oolemma (Flesch & Gadella, 2000; Naz & Rajesh, 2004; Senger, 2003).

At the beginning of the capacitation process, an efflux of cholesterol, and an influx of bicarbonate and calcium ions occur concomitantly. The influx of bicarbonate

causes the activation of adenylate cyclase (AC) responsible for the production of cyclic adenosine monophosphate (cAMP). Increased levels of cAMP then activate the AMP-dependent protein kinases (PKA), and subsequently induce protein tyrosine phosphorylation events. Active PKA pathways, along with the removal of cholesterol, also initiate changes in the plasma membrane such as the lateral redistribution of seminolipids and aminophospholipids into plasma membrane rafts (Flesch & Gadella, 2000). These changes result in an increase of membrane fluidity, which is essential for the spermatozoon to detach from the isthmus epithelium, to gain hyperactivated motility (sperm hyperactivation), and for proper acrosomal exocytosis to occur once it reaches the oocyte.

As aforementioned, a critical event that takes place during capacitation is the increase of intracellular calcium (Ca^{2+}). One method of Ca^{2+} entry into the sperm cell, is the through the CatSper Ca^{2+} channel localized near the flagellum. This channel is largely responsible for the hyperactivation found in viable spermatozoa (Kerns et al., 2018). CatSper is regulated by the HVCN1 channel, which itself, is negatively regulated by the presence of zinc ions (Zn^{2+}). It has recently been discovered that different signatures of Zn^{2+} distribution within sperm cells are associated with varying degrees of spontaneous sperm capacitation and fertility in livestock species (Kerns et al., 2018). This has been in part attributed to the need to remove inhibitory Zn^{2+}, such that the CatSper channels may become active and lead to an increase of intracellular Ca^{2+} (Flesch & Gadella, 2000).

Acrosomal exocytosis

Once a capacitated sperm cell reaches the oocyte, the next critical step is for that sperm cell to traverse the cumulus cell layers surrounding the oocyte and to bind to the zona pellucida (ZP). The bovine zona pellucida is composed of three glycosylated proteins: ZPA, ZPB, and ZPC (Gahlay et al., 2010; Gupta, 2021; Sutovsky, 2018). ZPB and ZPC are the proteins primarily responsible for initial sperm binding, the initiation of acrosomal exocytosis, and species specificity of sperm-oocyte interactions. ZPA is then involved in sustained binding capacity (Sutovsky, 2018).

The acrosomal matrix is encapsulated between outer and inner acrosomal membranes, form the apical ridge of the sperm head, including the equatorial segment (Yu et al., 2006). Once acrosomal exocytosis, formerly referred to as the acrosome reaction, has been initiated the outer acrosomal membrane (OAM) and the plasma membrane of the sperm head begin to fuse in such a way that many hybrid membrane vesicles arise, leading to the formation of the acrosomal shroud. This allows for cellular exocytosis of the acrosomal matrix, and exposes the inner acrosomal membrane (IAM) across the anterior sperm head, except at the equatorial segment (Yu et al., 2006). The spermatozoon is now able to penetrate the ZP via proteases found in the OAM, matrix, and IAM. Examples of these candidate proteases are acrosin, 26S proteasome (Yu et al., 2006) and membrane bound hyaluronidase (Flesch & Gadella, 2000). Once through the ZP, the sperm head's equatorial segment binds to microvilli of the oocyte's plasma membrane, termed the oolemma, via oolemma-binding proteins on the exposed equatorial segment (Flesch & Gadella, 2000; Senger, 2003; Sutovsky, 2018).

Gamete adhesion and fusion

Several candidate oolemma binding proteins have been identified in the equatorial segment of the spermatozoon and the oolemma of the oocyte, that are thought to be involved in gamete adhesion. Among them, IZUMO is the primary candidate protein found on the equatorial segment following acrosomal exocytosis and validated by gene ablation studies in the mouse. This protein is found only in male gametes and binds to JUNO, which is found on the oolemma (Hamze et al., 2020). Male IZUMO knock out (KO) mice have been found to be infertile, as their spermatozoa are unable to fuse with the oolemma. Oolemma protein JUNO is the candidate sperm receptor and IZUMO interactor during fertilization. Female JUNO KO mice are infertile, as their oocytes cannot be fertilized by wild type (WT) spermatozoa (Hamze et al., 2020). Following the incorporation of a spermatozoon into an oocyte, JUNO proteins are rapidly shed from the oolemma, suggesting a potential additive mechanism of anti-polyspermy defense (Bianchi et al., 2014). In addition to JUNO, it is hypothesized that CD9 and CD81 transmembrane domain proteins on the oolemma, also referred to as tetraspanins, are involved in sperm adhesion. Female CD9 KO mice are sub-fertile, and CD9-CD81 double KO mice are infertile (Benammar et al., 2017; Sutovsky, 2018). Tetraspanin proteins associate with other proteins within membrane rafts, and may contribute to the architecture of oocyte microvilli, which is instrumental for the adhesion and incorporation of the spermatozoon.

Oocyte activation and block to polyspermy

As the spermatozoon is engulfed by the oocyte, the post-acrosomal sheath on the caudal aspect of the sperm head dissolves, releasing the perinuclear theca contents into the oocyte's cytoplasm. The integration of perinuclear theca into the oocyte allows for

the sperm-borne oocyte activating factor (SOAF) to initiate oocyte activation, including anti-polyspermy defense, degradation of the cytostatic factor (CSF) responsible for meiotic metaphase II arrest, and the resumption of meiosis II. Although the true identity of the SOAF remains unknown, it is understood that it is a signaling molecule that induces oscillatory Ca^{2+} spikes derived from the oocytes ER, and leads to cortical granule exocytosis and pro-nuclear development in the oocyte (Campbell et al., 2000; Nomikos et al., 2013; Senger, 2003; Sutovsky, 2018).

One SOAF candidate is the post-acrosomal sheath WW domain-binding protein (PAWP/WBP2NL), which is found exclusively in the perinuclear theca of vertebrate spermatozoa (Sutovsky, 2018; Wu et al., 2007). This protein is transcribed, translated, and incorporated into the perinuclear theca during spermatid elongation. Experiments have shown that the injection of recombinant PAWP into metaphase II-arrested oocytes induces pronuclear development in various species, including porcine, bovine, macaque, and *Xenopus* (Wu et al., 2007). Additionally, the injection of a competitive peptide sequence or an anti-recombinant PAWP prevented the resumption of pronuclear development, therefore halting fertilization (Wu et al., 2007).

The currently favored SOAF candidate is a specific isoform of phospholipase-C, termed PLCζ or PLCZ1 (Nomikos et al., 2013). Studies using mouse and human samples have shown that the introduction of recombinant PLCζ into an oocyte leads to cleavage of the membrane bound phospholipid, phosphatidylinositol 4,5 bisphosphate (PIP_2), into membrane bound diacylglycerol (DAG) and soluble inositol 1,4,5- trisphosphate (IP_3). IP_3 then binds to receptors on the endoplasmic reticulum and causes the release of $Ca^{2+,}$ therefore resulting in the Ca^{2+} oscillations that are known to be necessary for oocyte

activation (Nomikos et al., 2013). It has also been observed that infertile human spermatozoa often have low levels of PLCζ, or have genetic mutations that result in dysfunctional PLCζ proteins (Nomikos et al., 2013). Although, there has been no homologue for this protein identified in the sperm of lower vertebrates such as amphibians.

Anti-polyspermy defense prevents more than one sperm cell from fusing with the oolemma, and is crucial for embryo survival (Susor et al., 2010). The first line of this defense comes from rapid membrane depolarization of the vitelline membrane/oolemma. But it is most effectively accomplished in mammalian oocytes via exocytosis of cortical granules (CG), termed the cortical reaction. During oocyte maturation, dense cortical granules begin to migrate towards the periphery of the oocyte cytoplasm in preparation for exocytosis into the perivitelline space (Senger, 2003). Once intracellular Ca^{2+} spikes lead to CG exocytosis, the granules release their contents, including ovastacin, which cleaves ZPB and initiates the zona block via zona hardening (Susor et al., 2010).

The cortical reaction process is regulated in part by the ubiquitin proteasome system (UPS), specifically by the ubiquitin C-terminal hydrolase-L1 (UCHL1) protein (Susor et al., 2010). The UPS regulates many cellular processes through rapid degradation of ubiquitin tagged proteins, and UCHL1 is one of the most abundant proteins found in bovine oocytes (Susor et al., 2010). Susor and others have shown that the inhibition of UCHL1 during oocyte maturation leads to altered translocation of the cortical granules and a resulting increase in polyspermy during fertilization (Mtango et al., 2012; Susor et al., 2010).

The increase in intracellular Ca^{2+} in the oocyte also controls the resumption of meiosis II, by regulating the removal of cytostatic factor (CSF) by anaphase-promoting complex (APC). Prior to oocyte activation by the fertilizing sperm cell, arrest at the metaphase II stage is achieved through high levels of cAMP and cGMP, which lead to the inactivation of the maturation-promoting factor (MPF) heterodimer (Pan & Li, 2019). MPF is composed of cyclin-dependent kinase 1 (CDK1) and cyclin B, and while in an inactive state, it maintains meiotic arrest (Pan & Li, 2019). Once APC is activated by an increase in Ca^{2+}, it ubiquitinates the cyclin B subunit of MPF and recruits the UPS to degrade cyclin B. This results in the activation of MPF and transition from metaphase II to anaphase II, which leads to completion of the second meiosis, extrusion of the second polar body and eventually maternal pronuclear development (Pan & Li, 2019).

Pronuclear development

Once the SOAF has caused oocyte activation and meiosis has resumed, the second polar body is extruded and the maternal pronucleus forms. For paternal pronuclear formation to occur, the sperm nucleus must undergo changes in the oocyte cytoplasm, markedly, the reduction of many disulfide bonds between protamine proteins that were incorporated into the sperm's nucleosomes during maturation in the epididymis (Collas & Poccia, 1998; Senger, 2003). High levels of glutathione present in the oocyte act to reduce the disulfide bonds, which allows the sperm chromatin to decondense (Senger, 2003). Concomitantly, as the chromatin decondenses, protamine proteins are rapidly replaced by oocyte-derived histones— initially by the linker H1FOO histone, followed by somatic cell-type histones H1-H4 (Gao et al., 2004).

As the sperm tail is being incorporated in the oocyte cytoplasm, the proximal centriole from the tail's connecting piece is released into the oocyte. The sperm-borne centriole is a component of the male germ cell's centrosome that undergoes reduction during spermiogenesis. The centrosome is a cell's microtubule organizing center (MTOC) composed of two centrioles and peri-centriolar material, and is primarily responsible for organizing cell division during mitosis and meiosis (Avidor-Reiss et al., 2020). The centriole itself is made of nine triplets of microtubules, arranged in a circular structure with a hollow center. Mature bovine spermatozoa contain one functional centriole, while the mature oocyte contains only peri-centriolar material (Avidor-Reiss et al., 2020). The centriole recruits the peri-centriolar material to form a sperm aster, which serves to bring the maternal and paternal pronuclei together to form pronuclear apposition that is critical for the first zygotic cleavage (Avidor-Reiss et al., 2020; Schatten & Sun, 2009). Once the pronuclei are brought together, the nuclear envelopes dissolve, allowing for maternal and paternal chromosomes to participate in the first zygotic cleavage divisions.

Early Embryonic Development

First cleavage divisions

Following successful fertilization, the newly formed bovine zygote will transition from the meiotic divisions of the oocyte to the first mitotic division of the diploid embryo by 30 hours post fertilization (HPF). Mitotic, cleavage divisions continue to proceed rapidly— halving the cytoplasmic content of each blastomere with each division, thus maintaining the original size of the embryo. During this time, maternal mRNAs support the embryo up until the embryonic genome activation (EGA) when the embryo acquires

the ability to produce its own transcripts (Memili & First, 1999). Prior to the major EGA event, maternal mRNAs begin to degrade (Graf et al., 2014; H. Wang & Dey, 2006). The mRNAs that translate to proteins that are used rapidly in the developing embryo, degrade faster due to a loss of RNA binding proteins which prevent the mRNA from being translated and degraded (Hentze et al., 2018).

Degradation of paternal mitochondria

All mammals inherit mitochondrial DNA (mtDNA) from their mother alone, meaning that paternally derived mitochondria must be disposed of during early embryo development. This is crucial for preventing mitochondrial heteroplasmy and is generally completed around the third cleavage division (Sutovsky et al., 1999, 2000). This process is mediated by two primary pathways: the UPS and autophagy (Sato & Sato, 2013; Song et al., 2016; Sutovsky et al., 2000). As previously discussed in this review, the UPS works to eliminate proteins that have been tagged for degradation via ubiquitin labeling and autophagy works to the same end via engulfment of ubiquitinated protein aggregates and organelle remnants by the autophagosome.

Ubiquitination of sperm mitochondria begins in the male reproductive tract, but the ubiquitin becomes masked by disulfide bonds while traversing the epididymis. This prevents eliciting the degradation response until after fertilization when disulfide bond reduction occurs in the oocyte cytoplasm (Sutovsky et al., 1999; Zuidema & Sutovsky, 2020). Immediately following fertilization, autophagy is enacted when autophagosomes begin to engulf sperm mitochondria and deliver them to lysosomes (Sato & Sato, 2013). Furthermore, previous literature has shown that these two processes have the capacity to work together to accomplish sperm mitochondrial degradation. For example, the

SQSTM1 autophagy receptor has the ability to recognize ubiquitinated mitochondrial proteins and bring them to interact with autophagosome proteins such as LC3 and GABARAP (Song et al., 2016). These processes must be efficient and effective to prevent mitochondrial heteroplasmy, which can lead to mitochondrial and neurodegenerative diseases (Stewart & Chinnery, 2015).

Embryonic genome activation

The EGA occurs in distinct waves, during different stages of development, depending on the species. In cattle, the major EGA occurs at the 8-16 cell stage, whereas in mice this occurs at the 2-4 cell stage, and in humans this occurs at the 4-8 cell stage (Graf et al., 2014). Epigenetic changes to the chromatin structure contribute to the initiation of this critical event. Methylated cytosines on DNA cause compact heterochromatin that is transcriptionally inactive, inverse to unmethylated cytosines which cause open euchromatin that is available to be transcriptionally active. Therefore, a global de-methylation event in the embryo genome is necessary to allow for the commencement of transcriptional activity (Arand et al., 2021; Bultman et al., 2006).

Pioneer transcription factors have a 3D structure that varies from that of other transcription factors, in that they are able to bind to DNA without disrupting the nucleosome, which therefore allows them to bind to condensed chromatin (Mayran & Drouin, 2018). These transcription factors are responsible for beginning to open compact embryonic chromatin and act upon the target DNA in two phases—first they bind rapidly, and second, they slowly stabilize the interaction. Slow stabilization may be related to nucleosomal changes that increase chromatin accessibility for second string transcription factors as well (Mayran & Drouin, 2018). Examples of pioneer transcription factors that

are important during the EGA are Oct4, Sox2, FoxA and Pax7 (Mayran et al., 2018; Mayran & Drouin, 2018).

Blastomere compaction

As cleavage continues, the blastomeres of the embryo now begin to experience different environments depending on if they are near the center of the embryo or located on the periphery, near the zona pellucida (Zernicka-Goetz et al., 2009). By the 8-16 cell stage of development, outer cells increase their contact with one another— causing compaction and the establishment of tight junctions between them, a hallmark of the developing embryo polarity (Nikas et al., 1996). Tight junctions form through the interaction of proteins such as occludin, claudin, ZO-1, and ZO-2 with cortical intracellular actin filaments to bind the cells together (Citi, 1993). Oriented by the tight junctions, these blastomeres evolve clear basolateral and apical domains, which will be necessary for blastocyst formation. The apical domain, facing the zona pellucida, is characterized by the presence of abundant microvilli (Citi, 1993). Although the inner cells also become compacted as cleavage continues and the embryo reaches the morula stage, they do not undergo the same polarization that the outer cells do (Citi, 1993; Zernicka-Goetz et al., 2009). This separation is one of the first events that leads to differential cell fates in the blastomeres that have all been totipotent up until this point.

Blastocyst formation

The compacted morula begins to transition to a blastocyst when fluid enters the embryo and becomes trapped inside, thus creating the blastocoel cavity. Sodium-potassium pumps (Na^+/K^+ -ATPase) are ATP dependent ion transporters located on the

basolateral membrane of the outer cells that will become committed to the trophectoderm (TE) lineage, and are responsible for the solute gradient inside the embryo (Madan et al., 2007; Violette et al., 2006). The Na^+/K^+-ATPase pumps actively transport Na^+ out of the cells and K^+ into the cells—therefore controlling the flow of water into the embryo to reach ionic equilibrium. Aquaporins located on both the basolateral and apical sides of the cells allow water to pass through the outer cells into the inner portion of the embryo (Barcroft et al., 2003). At this time, the blastocoel is created, and the embryo is now a called blastocyst.

Cell lineage commitments now continue through differential gene expression, and the Hippo signaling pathway is a key regulator of cell fate during blastocyst formation. When the Hippo signaling pathway is turned off, polarized cells on the periphery of the embryo begin to sequester LATS1/2 proteins at their apical domains, preventing them from acting freely in the cytoplasm. When LATS1/2 are bound together, they are unable to participate in the phosphorylation of Yes-associated protein 1 (YAP1) by protein kinases in the cytoplasm (Nishioka et al., 2009). The non-phosphorylated YAP1 now has the ability to enter the nucleus and bind to the transcription factor TEAD4, which induces transcription of caudal type homeobox 2 (CDX2) when active (Nishioka et al., 2009). The expression of CDX2 commits the peripheral, polar cells to becoming TE— which will further develop into extraembryonic membranes to become the placenta, tasked with supporting the fetus during gestation (Nishioka et al., 2009; Zernicka-Goetz et al., 2009). Conversely, when the Hippo signaling pathway is turned on, non-polar cells in the center of the embryo do not bind LATS1/2 proteins due to lacking apical domains, which allows them to participate in the phosphorylation of YAP by protein kinases in the cytoplasm.

Phosphorylated YAP (P-YAP) is unable to enter the nucleus to activate TEAD4, therefore preventing the expression of CDX2 (Nishioka et al., 2009). At this point in development, these cells are considered the pluripotent inner cell mass (ICM) and are marked by the expression of OCT4, at least in murine embryos (Zernicka-Goetz et al., 2009). In bovine embryos, it is still not well understood what marks these cells as the ICM, aside from the absence of CDX2 (Ortega et al., 2020; Pfeffer, 2018). Altogether, these events constitute the first cell lineage commitment.

Following the first cell lineage commitment, the cells of ICM segregate again via differential gene expression and commit to either the hypoblast or epiblast lineage. In cattle, the hypoblast is marked by expression of NANOG, and the epiblast is marked by expression of OCT4 and SOX2 (Ortega et al., 2020; Pfeffer, 2018).

Cellular Stress in the Early Embryo

Reactive Oxygen Species

Reactive oxygen species (ROS) are molecules derived from molecular oxygen that have an increased ability to oxidize other molecules that they encounter. These molecules can be formed by reduction-oxidation (redox) reactions, as well as participate in them (Sies & Jones, 2020). During a redox reaction, one molecule (the reducing agent) loses electrons and becomes oxidized while the other molecule (the oxidizing agent) gains electrons and becomes reduced. Some ROS are free radicals—meaning that they contain an unpaired electron which makes them highly reactive. Examples of free radicals are superoxide ($O_2^{\cdot}$), hydroxyl ($OH^{\cdot}$), and peroxyl ($RO_2^{\cdot}$) (Bayr, 2005). Other ROS are considered nonradical oxidizing agents, lacking an unpaired electron but having

increased reactivity and a greater potential to form free radicals. Examples of nonradical oxidizing agents are hydrogen peroxide (H_2O_2) and ozone (O_3) (Bayr, 2005).

A primary source of intracellular ROS production is the electron transport chain of the mitochondria during oxidative phosphorylation. During this process, molecular oxygen is the final electron acceptor, which can produce ROS when oxygen is only partially reduced to the superoxide radical (Kuznetsov et al., 2011). Additionally, ROS are produced via signal transduction, transcription factor activation, and other enzymatic reactions; as well as in response to external factors such as UV radiation, heat stress, starvation, and more (Bayr, 2005).

Reactive oxygen species are inherent to normal cellular function and metabolism. Specifically, H_2O_2 is recognized to be biologically ubiquitous in the regulation of redox reactions (Sies & Jones, 2020). Hydrogen peroxide was first discovered to be present at steady physiological levels in normal respiring eukaryotic cells in 1970 (Sies & Chance, 1970). Additionally, it was discovered that catalase compound I, which has the potential to reduce H_2O_2, was also present in steady levels in eukaryotic cells (Sies & Chance, 1970). ROS are involved in cell signaling pathways such as the transcription factor nuclear factor- κB (NF- κB) pathway, which regulates transcription of inflammatory associated genes (Sies & Jones, 2020). Although ROS molecules are necessary for cellular function at physiological levels, they can also be damaging at increased concentrations due to their ability to oxidize cellular components such as nucleic acids, lipids and proteins.

High concentrations of ROS—often produced in response to cellular stressors such as heat stress, starvation, hypoxia, and toxic agents—can lead to oxidation of DNA,

lipids, and proteins (Cavallari et al., 2019; Kuznetsov et al., 2011). Levels of ROS are generally controlled by antioxidants such as such as superoxide dismutase (SOD), catalase, glutathione peroxidase, glutathione, and ascorbate (vitamin C) which have the ability to donate electrons without becoming unstable (Bayr, 2005). When antioxidants are no longer able to balance the activity of ROS, cells undergo oxidative stress and cellular damage occurs. DNA damage due to oxidation can be in the form of DNA base damage, double or single strand breaks, or 8-hydroxylation of guanine. Polyunsaturated fatty acid side chains of membrane phospholipids are especially sensitive to oxidation and affect membrane fluidity if attacked (Bayr, 2005).

The damaging effects of oxidative stress have been linked to developmental failure in early embryos. In human embryos, it has been found that levels of H_2O_2 are significantly higher in those that undergo fragmentation and apoptosis than those that do not. This suggests a direct correlation between H_2O_2 concentration and cell death (Yang et al., 1998). In murine embryos, it was shown that there is an increase in ROS production around the 2 cell stage, which coincided with embryo arrest in that study (Nasr-Esfahani & Johnson, 1991). In the bovine, a reduction in oocytes that developed to the blastocyst stage was correlated with increased ROS and decreased glutathione levels (Hashimoto et al., 2000). It has also been observed that ROS levels fluctuate in fertilized bovine oocytes, with significant peaks at 7, 19 and 24 hours post fertilization (Morado et al., 2013).

The function of ROS in cellular metabolism and signaling is essential for all cells, including the blastomeres of developing embryos which undergo dramatic changes throughout the first week of development. Although, if left unregulated by antioxidants,

ROS may lead to damaging oxidative effects on blastomeres as well. Research continues to investigate the diverse roles of ROS and how they may be implemented during early embryonic development.

Endoplasmic reticulum stress

The endoplasmic reticulum (ER)—composed of both the rough ER, which is covered in ribosomes, as well as smooth ER, which lacks ribosomes—is an organelle involved in protein synthesis and folding. Within the ER lumen, proteins are modified and folded via disulfide bond formation, glycosylation, and chaperone-mediated folding prior to achieving their functional states and being sent to their intended locations in the cell (Zeeshan et al., 2016). Correct posttranslational protein modification is assured by the endoplasmatic reticulum associated degradation (ERAD) machinery, a quality control mechanism that recognizes misfolded proteins and tags them with ubiquitin for proteasomal degradation. Additionally, the ER serves as a storage center for Ca^{2+} and is involved in many intracellular signaling cascades (Banhegyi et al., 2007).

Disruption in cellular homeostasis often impacts the functionality of the ER and may lead to an accumulation of misfolded, aggregated proteins in the ER lumen (Banhegyi et al., 2007; Michalak & Gye, 2015). This state then leads to the activation of multiple processes referred to as the unfolded protein response (UPR), which allows the cell to either promote survival and mitigate deleterious impacts or lead to apoptosis. One pro-survival pathway involves the abundant ER chaperone, 78-kDa glucose-regulated protein (GRP78), which may also be referred to BiP or HSPA5 in the literature (Banhegyi et al., 2007; M. Wang et al., 2009; Zeeshan et al., 2016). During times of basal functionality, GRP78 is instrumental in the folding, formation, and quality control

of newly synthesized proteins. Additionally, GRP78 is a quality control regulator during the UPR as well. In the mouse, it has been demonstrated that embryos depleted of GRP78 lack the ability to hatch from the zona pellucida and therefore undergo embryo mortality around day 3.5 (Banhegyi et al., 2007).

The unfolded protein response is also linked to other stress-induced pathways such as the production of ROS (Yoon et al., 2014; Zeeshan et al., 2016) and autophagic activity (Song et al., 2012). Both ER stress and ROS production are fundamental processes associated with UPR, and there is evidence of increased ROS appearing to initiate UPR (Zeeshan et al., 2016). Furthermore, it has been demonstrated that the ER can contribute to ROS production. The literature has suggested that the membrane-bound protein—endoplasmic reticulum oxidoreductin-1 (ERO1) has the ability to oxidize the luminal chaperone protein—protein disulfide isomerase (PDI), disrupting its normal role in preventing protein aggregation (Zeeshan et al., 2016).

In preimplantation bovine embryos, exposure to high concentrations of atmospheric oxygen increased ROS production (de Castro e Paula & Hansen, 2008) and subsequently, increased the expression of ER stress markers such as sXBP-1, and the percent of apoptotic cells (Yoon et al., 2014). This phenotype resulted in decreased blastocyst rates, but when the cooperative action between ROS and ER stress was disrupted, blastocyst rates could be rescued (Yoon et al., 2014). Similarly, when the process of autophagy is induced in bovine embryos, ER stress was alleviated and blastocyst rates improved (Song et al., 2012).

Autophagy

Autophagy is a cellular recycling mechanism in which proteins and organelles that are no longer necessary or functional can be degraded in the lysosome, allowing their subsequent byproducts to be reused (Cecconi & Levine, 2008; Mizushima, 2007). There are three types of autophagic activity: microautophagy, macroautophagy, and chaperone-mediated autophagy (Cecconi & Levine, 2008; Mizushima, 2007). These differ in the way that targeted proteins and organelles enter the lysosome for degradation. Macroautophagy is the primary method of autophagy in mammalian cells, and is generally referred to simply as "autophagy" in the literature (Mizushima, 2007).

During the process of autophagy, targeted proteins and organelles are engulfed by a temporary structure—the autophagosome—before being brought to the lysosome for enzymatic hydrolysis. The autophagosome is composed of the 18 different Atg proteins: Atg1-10, Atg12-14, Atg16-18, Atg29, and Atg31 (Mizushima, 2007). The congregation of these proteins then recruits microtubule-associated protein 1 light chain 3 (LC3) from the cytoplasm in the form of LC3-I, to bind with the forming autophagophore complex. This converts LC3-I into the membrane bound form, LC3-II, and leads to the completion of forming the fully, enclosed, double membrane autophagosome vesicle (Balboula et al., 2020). The fully formed autophagosome will then be promoted by phosphatidylinositol 3-kinase (PI3K) to fuse with the lysosome, creating a structure termed the autolysosome, and engulfed targets will be degraded by hydrolysis.

The process of autophagy is crucial during embryo development. Examples of routine events in the early embryo wherein autophagic activity has been observed are during the time of fertilization, the degradation of paternal mitochondria, and the degradation of maternal components during the maternal to embryonic transition (Song et

al., 2016; Tsukamoto et al., 2008). Previous literature has shown, through the measurement of LC3-II abundance, that autophagy is much more active in fertilized zygotes than in unfertilized oocytes (Tsukamoto et al., 2008). Following sperm penetration, an upregulation in PI3K signaling pathway has been observed in zygotes, which is known to promote fusion of the autophagosome with the lysosome and was correlated with levels of autophagic activity in early embryos (Yamamoto et al., 2014).

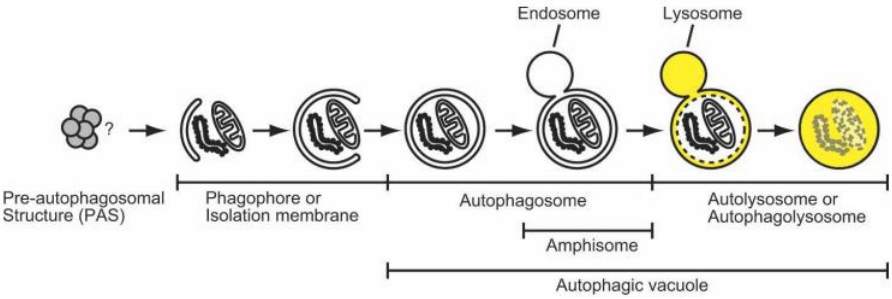

Figure 1.5.1 Autophagic pathway. Adapted from Mizushima, N., 2007.

Autophagy, in conjunction with the UPS, is important for the degradation of the paternal mitochondria, and is termed sperm mitophagy in this scenario (Song et al., 2016). This process is crucial to ensure successful preimplantation development and to prevent mitochondrial diseases arising from heteroplasmy. Autophagy continues to play a role in early embryo development by supporting the transition from using maternal derived transcripts, by degrading them and allowing their amino acids to be recycled for embryonic use. Murine zygotes that lack autophagic activity due to a loss of protein Atg5 in both the oocyte and the spermatozoa undergo apoptosis by the 4-8 cell stage of development (Tsukamoto et al., 2008). This study, as well as others (Balboula et al.,

2020), provide evidence that the autophagic pathway is essential for embryo survival to the blastocyst stage.

Although autophagy is involved in routine maintenance events during embryo development, it is also known to be upregulated during times of cellular stress such as cell starvation, ER stress, and hypoxia (Mizushima, 2007). Due to recycling unnecessary cellular components, this process is used as a pro-survival mechanism and works to mitigate the deleterious impacts of cellular stress. During ER stress, a cell accumulates an increased abundance of misfolded and aggregated proteins, which must be degraded for normal cellular function to proceed, resulting in the upregulation of the autophagic pathway (Ravanan et al., 2017). It has been demonstrated that the induction of autophagy can alleviate impacts of ER stress in embryos, and inversely, the defects found in autophagy-inhibited embryos can also be alleviated if treated with an ER stress inhibitor as well (Song et al., 2012).

Gap in Knowledge

Given the information reviewed here, there is an outstanding need to elucidate the relationship between sire fertility, morphological and functional characteristics of spermatozoa that may impact the preimplantation embryo, and cellular stress in early embryonic development. This will lead to a deeper understanding of how variation in sire fertility impacts cellular stress mechanisms, and ultimately embryo viability, in the early embryo. Additionally, this would allow for the identification of characteristics of spermatozoa quality that can be correlated with embryo development, independent of SCR.

Chapter 2: Paternal Contributions to Early Embryonic Stress in the Bovine

Introduction

Pregnancy loss is one of the primary contributors to economic failure in the dairy cattle industry (Cerri et al., 2009; Diskin & Morris, 2008; Maurer & Chenault, 1983; Wiltbank et al., 2016). Pregnancy loss can be classified under two predominant categories: early pregnancy loss which occurs between days 1-27 and late pregnancy loss which occurs from day 28 throughout gestation (Wiltbank et al., 2016). As gestation continues, the probability of pregnancy loss decreases. The early pregnancy loss period is further divided into loss occurring during days 1-7 and days 8-27 of development. By day 7, up to 50% of all embryo mortality will have already occurred, and between days 8-27, up to 36% of embryo mortality may occur (Wiltbank et al., 2016).

The first week following fertilization is a critical time for embryo development and survival. Events such as the first cellular divisions— cleavage, embryonic genome activation, clearance of paternal mitochondria, cell polarization and compaction, and cell lineage specifications are all crucial steps for embryo survival (Figure 2.1) (Graf et al., 2014; Memili & First, 1999; van Soom et al., 1997). If an embryo is unable to complete any of these steps, it will arrest.

Poor quality oocytes are known to result in decreased developmental competence of subsequent embryos. For an oocyte to be prepared for fertilization and to support early embryo development, it must undergo successful cytoplasmic and nuclear maturation (Krisher, 2003). A few examples of contributions to oocyte quality include the

accumulation of messenger RNA (mRNA) transcripts prior to fertilization, proper cortical granule exocytosis following fertilization, and the completion of meiosis II following oocyte activation (Krisher, 2003; Senger, 2003). The accumulated mRNA will sustain embryo development through the first few cleavage divisions, while the embryo is transcriptionally quiescent, prior to the embryonic genome activation (Krisher, 2003; Memili & First, 1999; Stitzel & Seydoux, 2007). Proper cortical granule exocytosis prevents the occurrence of polyspermy, and the completion of meiosis is crucial for maternal pronuclear development prior to the first embryonic division (Senger, 2003). These are examples of the many maternal contributions that have been extensively studied in early embryos, although historically, there has been less focus on the paternal contributions to these events.

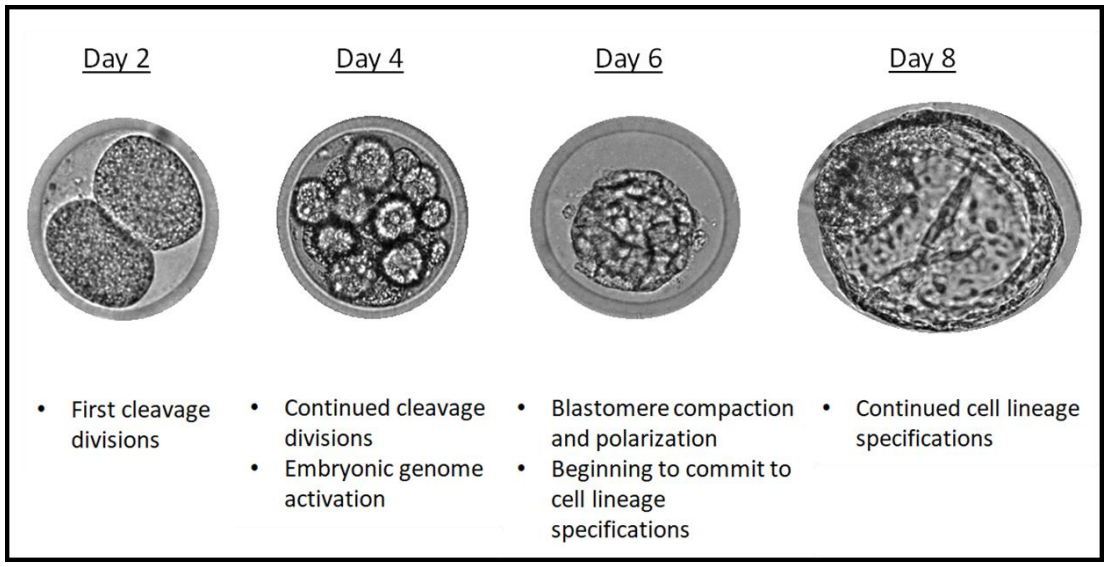

Figure 2.1. Critical timepoints in early embryo development.

There is evidence that the sire exhibits its greatest impact on pregnancy success during the events of fertilization, early embryo development, and conceptus elongation (Ortega et al., 2018). Remarkably, the spermatozoon begins regulating embryo viability

immediately following penetration of an oocyte. By releasing its sperm-borne oocyte activating factor (SOAF**),** the spermatozoon initiates oocyte activation, including anti-polyspermy defense and the completion of meiosis II (Campbell et al., 2000; Nomikos et al., 2013; Sutovsky, 2018). This is followed by decondensation of the paternal chromatin and the contribution of the sperm-derived centriole—both of which are critical for the first cleavage division (Avidor-Reiss et al., 2020; Schatten & Sun, 2009; Sutovsky et al., 1996). Previous work in our lab has shown that commercial AI sires differ in their ability to produce viable blastocysts in an *in vitro* culture system (Lockhart et al., submitted JDS.2022), yet our understanding of the malfunction of cellular mechanisms regulated by sire during early embryo development is still lacking. Elucidating these mechanisms that are influenced by sire will lead to a deeper understanding of early embryo mortality, as well as the development of new biomarkers of sperm fertility and early embryonic development.

Cellular stress mechanisms have been identified as key regulatory elements that may be impacted by sire variation. Sires with decreased ability to produce blastocysts (classified as low performing) were found to produce embryos that have increased autophagic activity, as well as an increase in embryo arrest at the 2-6 cell stage of development (Lockhart et al., submitted JDS.2022). Autophagy is a cellular recycling mechanism that degrades targeted proteins and organelles and allows for the subsequent byproducts to be re-used (Mizushima, 2007; Song et al., 2012). Autophagic activity is also known to be upregulated during times of cellular stress such as the response to misfolded proteins and cell starvation (Song et al., 2012).

Another mechanism that is upregulated during times of stress is the production of reactive oxygen species (ROS)—molecules derived from molecular oxygen that have an increased ability to oxidize other molecules that they encounter (Bayr, 2005; Sies & Jones, 2020). Reactive oxygen species are primarily produced in the mitochondria during oxidative phosphorylation and, although vital at low concentrations, are commonly increased and become pathological when a cell is under stress (Kuznetsov et al., 2011). High levels of intracellular ROS can damage the cell and lead to DNA damage, lipid oxidation, and endoplasmic reticulum (ER) stress which causes the unfolded protein response and disrupts cellular proteostasis (Bayr, 2005; Guerin, 2001; Kuznetsov et al., 2011).

This leads to the hypothesis of the current study—that embryos produced by low performing sires have increased autophagic activity in response to an increase in cellular stress and ROS production, compared to embryos produced by high performing sires, therefore resulting in impaired development. The first aim of this study was to characterize the autophagic activity and ROS production of embryos produced by high performing and low performing sires under both normal culture conditions and induced stress conditions. The second aim was to evaluate mechanisms that may be impacted downstream from cellular stress such as DNA damage and lipid oxidation in preimplantation bovine embryos.

Materials and Methods

Embryo production

All media for oocyte collection and maturation, as well as *in vitro* embryo production, were prepared as previously described (Ortega et al., 2017, 2018). Briefly, cumulus-oocyte complexes (COCs) were collected from abattoir derived ovaries. COCs with at least three layers of compact cumulus cells and homogeneous cytoplasm were selected and placed in oocyte maturation medium warmed to 38.5°C and equilibrated with air containing 5% (v/v) CO_2. Oocytes, in groups of 50, were left to mature for approximately 22 hours prior to fertilization. Semen straws used in all experiments were gifted by Select Sires Inc. (Great Plains, OH) and were processed in the same commercial house. Semen was collected from Holstein sires at approximately 28 months of age on average. Up to four high performing sires and four low performing sires were selected for the experiments of this study based on previous classification as having high or low capacity to produce embryos (Lockhart et al., submitted JDS.2022.). Spermatozoa were prepared for fertilization as previously described (Ortega et al., 2017, 2018) and diluted in fertilization medium (IVF-TALP) to a final concentration of $1x10^6$/ml in the fertilization plate. Mature oocytes and spermatozoa were incubated together for 18-20 hours at 38.5°C with air containing 5% (v/v) CO_2, following which, cumulus cells were removed, and putative zygotes were placed in synthetic oviductal fluid (SOF-BEII) culture medium in a controlled environment (38.5° C with a humidified atmosphere of 5% (v/v) CO_2, 5% (v/v) O_2, 90% (v/v) N_2). Cleavage rates were assessed on the third day of embryo culture (66-72 hours post insemination [HPI]) and blastocyst rates were assessed in the morning on the eighth day of embryo culture (186-192 HPI). Developmental data were collected over the course of 47 replicates and analyzed using a generalized linear mixed model in Statistical Analysis System (SAS) version 9.4 (SAS

Institute Inc., Cary, NC) and are expressed as least squares means (LS means**)** ± standard error mean (SEM).

Fertilization rate

A total of 117-130 putative zygotes per sire classification were collected at 18-20 HPI, over the course of four replicates. Putative zygotes were stripped of cumulus cells both with mechanical motion, as well as treatment with pronase (Thermo-Fisher Scientific) for 60 seconds. They were then washed three times in phosphate-buffered saline with polyvinylpyrrolidone **(**PBS-PVP: 1 mg PVP per 1mL of 1x PBS), fixed in 4% paraformaldehyde for 15 minutes at room temperature, and washed three more times in PBS-PVP. Putative zygotes were then incubated with Hoechst 33342 nuclear stain (Thermo-Fisher Scientific) at a concentration of 1 µg/mL, diluted in PBS-PVP, for 15 minutes before being mounted on glass slides with 6 µL of slow fade gold antifade solution (Thermo-Fisher Scientific). Slides were imaged on a Leica DM5500 B fluorescent microscope with an attached Leica DFC450 C camera at the pro-nuclear stage to assess the fertilization rate. Zygotes containing two pronuclei were considered successfully fertilized. Then, data were analyzed with a binomial logistic regression model, using the GLIMMIX procedure in SAS. LS means and SEM were identified using the pdiff option of LSMEANS.

Autophagy and ROS under normal conditions

A total of 60-80 embryos per stage, per fertility classification were collected at four stages of development— 2-6 cell (30-55 HPI), 8-16 cell (60-75 HPI), morula (120-144 HPI), and blastocyst (168-192 HPI) over the course of three replicates and co-stained

to assess both autophagy and ROS production in each live embryo. Autophagosomes were labeled using the Cyto-ID Autophagy Detection Kit 2.0 (Enzo Life Sciences) as previously described (Chan et al., 2012), and ROS were labeled using CellROX Deep Red Reagent (Thermo-Fisher Scientific). Briefly, 1 µL of Cyto-ID Green Autophagy Stain was added to 500 µL of the provided assay buffer, and 0.5 µL of that mixture was added to 250 µL of SOF-PVP (1 mg PVP per 1 mL SOF-BEII) warmed to 38.5°C. CellROX Deep Red Reagent was also diluted in warm SOF-PVP to a 10 µM concentration. Then, 80 µL of each stain was added to a 96-well plate and mixed thoroughly. Embryos were washed three times in warm SOF-PVP, then placed into stain mixture and incubated for 25 minutes at 38.5° C in a humidified atmosphere of 5% (v/v) CO_2, 5% (v/v) O_2, 90% (v/v) N_2. Following incubation, embryos were immediately washed again in warm SOF-PVP and mounted on glass slides in 6 µL of antifade solution (Thermo-Fisher Scientific). All embryos were imaged under identical illumination and exposure settings on a Leica DM5500 B fluorescent microscope with an attached Leica DFC450 C camera. Mean fluorescent intensity (MFI) of each image was measured using ImageJ Software. MFI was calculated by subtracting the mean background intensity from the mean embryo intensity, on each channel individually. The ROS-induced fluorescence was measured at 590 nm wavelength in the TRITC channel and autophagy was measured at 510 nm wavelength in the FITC channel. Data were analyzed using a generalized linear mixed model in SAS and are expressed as LS means ± SEM.

Autophagy and ROS under stress conditions

Following the removal of cumulus cells via mechanical motion during in vitro embryo production, zygotes were randomly assigned to the treatment group or control

group. Treatment embryos were exposed to heat stress at 41°C for four hours before being placed in normal culture conditions (38.5° C with a humidified atmosphere of 5% (v/v) CO_2, 5% (v/v) O_2, 90% (v/v) N_2). Heat stress temperature was chosen based on previous literature (Al-Katanani & Hansen, 2002). Control embryos were placed directly into normal culture conditions. A total of 60-80 embryos per stage, per fertility classification were collected at the 2-6 cell stage of development (30-55 HPI) over the course of four replicates and co-stained to assess both autophagy and ROS production. Staining, imaging, and data analysis for autophagic activity and ROS production was performed as in the previous experiment. Developmental data for this experiment were analyzed including cleavage rates recorded from IVF replicates that produced embryos to be collected at the 2-6 cell stage for staining, and therefore do not have corresponding blastocyst rates. Developmental data were analyzed using a generalized linear mixed model in SAS and are expressed as LS means ± SEM.

DNA damage

A total of 108-135 embryos per fertility classification were collected at the 2-6 cell stage (30-55 HPI) over the course of three replicates and stained by using the In Situ Cell Death Detection kit (Roche Diagnostics) to assess the presence of DNA fragmentation in each embryo. Embryos were washed three times in PBS-PVP, fixed in 4% paraformaldehyde for 15 minutes at room temperature, washed again three times, and permeabilized in permeabilization solution (0.5% Triton X-100 diluted in PBS) for 40 minutes at room temperature. TUNEL solution was prepared by adding 15 µL of the provided enzyme to 135 µL of the label solution. For each replicate, 3-5 embryos were prepared to serve as positive controls, and 3-5 were set aside for negative controls.

Positive control embryos were incubated in 8 µL of DNAse for ten minutes prior to adding 25 µL of the TUNEL solution. At that time, embryos were place in either a negative control group (into 25 µL the label solution only) or placed into 25 µL of prepared TUNEL solution and both were incubated for 1 hour at 38.5° C in a humidified atmosphere of 5% (v/v) CO_2, 5% (v/v) O_2, 90% (v/v) N_2. Following incubation, all embryos were washed three times in PBS-PVP and placed into Hoechst 33342 nuclear stain (Thermo-Fisher Scientific) at a concentration of 1 µg/mL, diluted in PBS-PVP, for 15 minutes. Embryos were then mounted on glass slides with antifade solution (Thermo-Fisher Scientific) and imaged under identical lighting conditions on a Leica DM5500 B fluorescent microscope with an attached Leica DFC450 C camera. The presence or absence of DNA fragmentation was recorded, and data were analyzed with a binomial logistic regression model, using the GLIMMIX procedure in SAS. Means and SEM were identified using the pdiff option of LSMEANS.

Lipid Oxidation

A total of 108-130 embryos per fertility classification were collected at the 2-6 cell stage (30-55 HPI) over the course of six replicates and stained with the Image-iT™ Lipid Peroxidation Kit (Thermo-Fisher Scientific) to quantify the percentage of oxidized lipids in each live embryo. Lipid peroxidation stain was used according to manufacturer's recommendations. Embryos were washed three times in SOF-PVP warmed to 38.5°C before 3-5 were set aside to be positive controls. To prepare the positive control, 1 µL of the provided cumene hydroperoxide was diluted in 54 µL of pure ethanol, and then 0.5 µL of this stock solution was added to 500 µL of 1x PBS for a final concentration of 100 mM. Embryos assigned to the positive control group were

added to 100 µL of this solution for 10 minutes at 38.5°C. The lipid peroxidation stain was diluted to a 10 µM concentration in warm 1x PBS-PVP. At this time, all embryos were placed into the stain and incubated for 30 minutes at 38.5° C with a humidified atmosphere of 5% (v/v) CO_2, 5 % (v/v) O_2, 90 % (v/v) N_2. Following incubation, embryos were immediately washed again three times in warm SOF-PVP, mounted on glass slides in 6 µL of antifade solution (Thermo-Fisher Scientific), and imaged on a Leica DM5500 B fluorescent microscope with an attached Leica DFC450 C camera. To quantify the percentage of lipids oxidized, the MFI of each embryo was measured using ImageJ Software. All lipids were measured at 590 nm wavelength in the TRITC channel and oxidized lipids were measured at 510 nm wavelength in the FITC channel, with the background fluorescence subtracted from the embryo fluorescence, before dividing the oxidized lipid value by the total lipid value for a final percentage. Data were then analyzed using a generalized linear mixed model in SAS and are expressed as LS means ± SEM.

Results

Fertilization rates and embryo development

Putative zygotes were determined to be successfully fertilized by the presence of two pro-nuclei at 18-20 HPI (Figure 2.2A). The fertilization rates of each fertility classification (n=117-131) are shown in Figure 2.2B. There was no significant difference observed between high (77.86% ± 3.62%) and low (74.78 ± 4.05%) performing sires (*P*=0.571). Cleavage and blastocyst rates are shown in Figure 2.2C, D. Cleavage rates from embryos produced by high performing sires (76.73% ± 2.57%) were significantly

higher (*P*= 0.029) than cleavage rates from low performing sires (68.25% ± 2.74%). Similarly, blastocyst rates from embryos produced by high performing sires (29.04% ± 1.78%) were significantly higher (*P*= 0.001) than blastocyst rates from low performing sires (19.94% ± 1.90%).

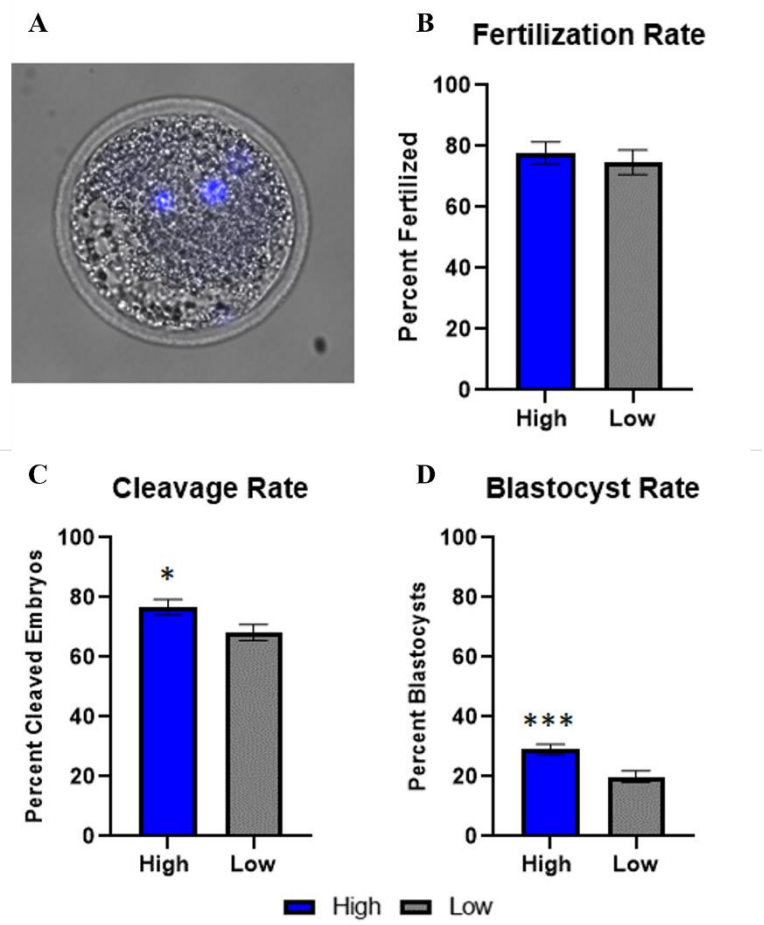

Figure 2.2. Fertilization rate and embryonic development. (A) Representative image of a zygote containing both paternal and maternal pronuclei just prior to pronucelar apposition. (B) No difference was observed (*P*=0.571) between high performing and low performing sires' ability to successfully fertilize oocytes (n=117-131). (C, D) Embryos produced by high performing sires had significantly higher cleavage rates (*P*=0.029) and blastocyst rates (*P*=0.001) than embryos produced by low performing sires (n=47 *in vitro* fertilization replicates).

Autophagy and ROS under normal conditions

When comparing the ROS production and autophagic activity of embryos produced from either high or low performing sires, under normal culture conditions, the most striking differences were observed at the 2-6 cell stage of development (Figure 2.3B, C). Embryos at the 2-6 cell stage, produced by low performing sires exhibited an increase in both ROS production (21.89 ± 0.79) and autophagic activity (13.28 ± 0.47) compared to embryos from high performing sires (16.18 ± 0.94, $P<0.0001$; 11.28 ± 0.56, $P=0.007$), respectively. Embryos at the morula stage, produced by low performing sires also exhibited an increase ($P=0.009$) in ROS production (22.45 ± 1.23) compared to embryos from high performing sires (18.16 ± 1.09), but no corresponding increase in autophagy was observed. There were no significant differences observed between the groups at the 8-16 cell or blastocyst stages of development ($P>0.05$).

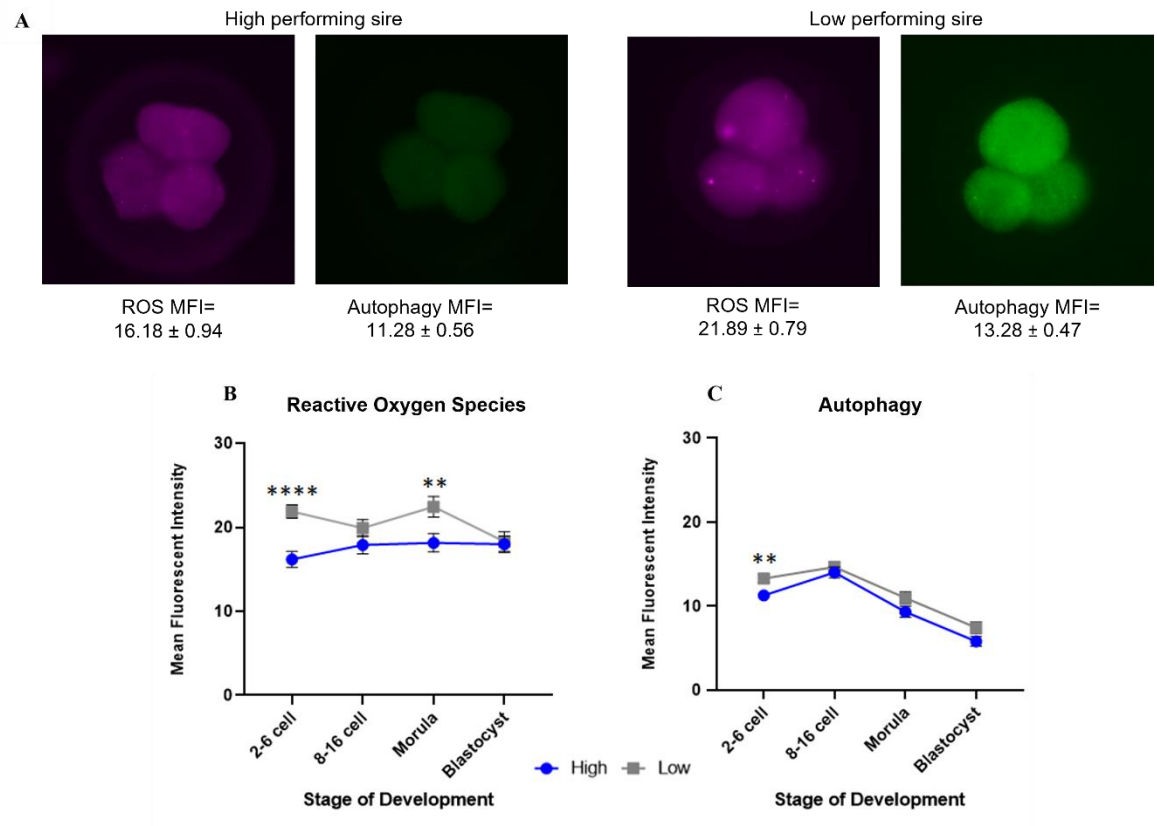

Figure 2.3. Autophagy and ROS production under normal culture conditions. (A) Representative images of the 2-6 cell stage in embryos from high performing sires (left) and low performing sires (right). Fluorescence emitted from ROS activity is shown in magenta and fluorescence emitted from autophagic activity is shown in green. Mean fluorescent intensity (MFI) for each process is listed below the corresponding image. (B) 2-6 cell and morula stage embryos produced by low performing sires had significantly increased *(P*<0.0001; *P*=0.009*)* ROS production compared to embryos produced by high performing sires (n=60-80 embryos per stage, per classification). (C) 2-6 cell embryos produced by low performing sires had significantly increased (*P*=0.007) autophagic activity compared to embryos produced from high performing sires (n=60-80 embryos per classification).

Autophagy and ROS under stress conditions

To assess the impact of induced stress on embryos from each group, ROS production and autophagic activity were compared at the 2-6 cell stage of development, and cleavage and blastocyst rates were recorded (Figure 2.4). Embryos at the 2-6 cell stage produced by low performing sires under heat stress had increased ROS production (25.52 ± 0.62) when compared to embryos produced by high performing sires under heat stress (21.68 ± 0.82; P=0.0002), embryos from low performing sires under normal conditions (22.31 ± 0.52; P<0.0001), and embryos from high performing sires under normal conditions (20.29 ± 0.56; P<0.0001). Additionally, the ROS production from embryos produced by low performing sires under normal conditions was significantly increased when compared to embryos produced by high performing sires under normal conditions (P=0.0086). Alternatively, 2-6 cell embryos produced by high performing sires under heat stress had increased autophagic activity (25.53 ± 3.41) when compared to embryos from low performing sires under normal conditions (15.30 ± 2.16; P=0.0117) and embryos from high performing sires under normal conditions (13.74 ± 2.35; P=0.0046). Cleavage rates from embryos produced by high performing sires cultured under normal conditions (70.74% ± 2.71%), were significantly higher (P=0.015) than cleavage rates from embryos produced by low performing sires cultured under heat stress (57.95% ± 4.37%). There was no difference in blastocyst rate observed between embryos of any group (P>0.05).

DNA damage

The DNA damage present in embryos produced from high and low performing sires is shown in Figure 2.5A. There was no difference (P=0.334) in the percent of

TUNEL positive cells in embryos produced from high performing sires (6.72% ± 2.16%) when compared to embryos produced from low performing sires (10.19% ± 2.91%).

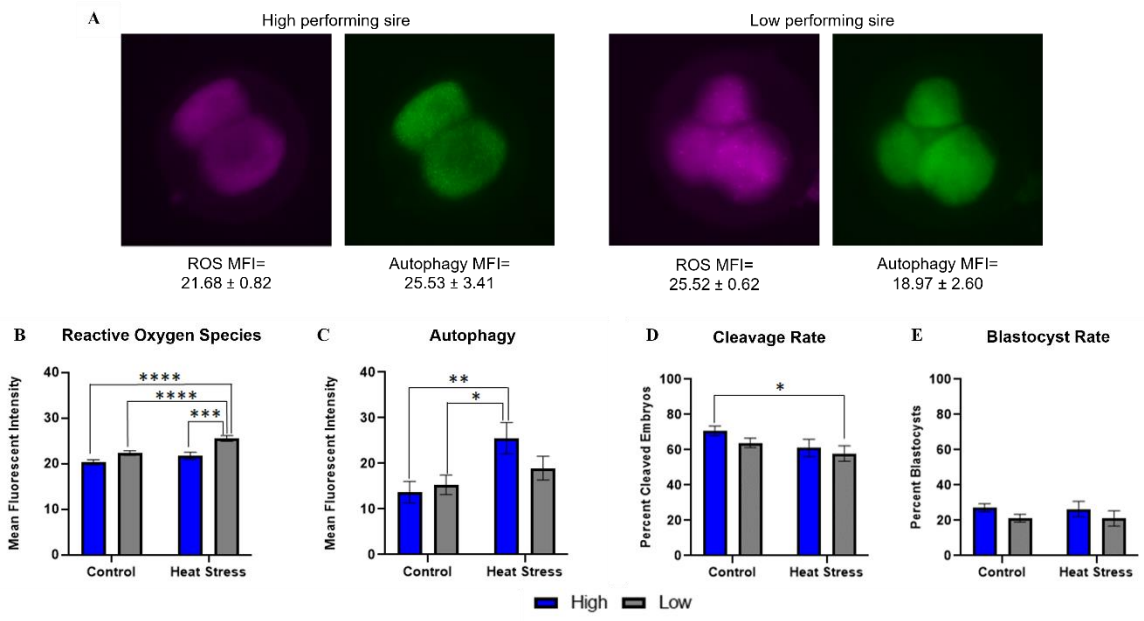

Figure 2.4. Autophagy and ROS production under induced heat stress. (A) Representative images of 2-6 cell, heat stressed embryos from high performing sires (left) and low performing sires (right). Fluorescence emitted from ROS activity is shown in magenta and fluorescence emitted from autophagic activity is shown in green. Mean fluorescent intensity (MFI) for each source is listed below the corresponding image. (B) 2-6 cell embryos produced by low performing sires under heat stress, had increased ROS production compared to all other embryos– from high performing sires under heat stress (P=0.0002), from low performing sires under normal conditions (P<0.0001), and from high performing sires under normal conditions (P<0.0001). Additionally, embryos produced by low performing sires under normal conditions had increased ROS production when compared to embryos produced by high performing sires under normal conditions (P=0.0086) (n=60-80 embryos per classification). (C) 2-6 cell embryos produced by high performing sires under heat stress had increased autophagic activity when compared to embryos from either high (P=0.0117) or low performing sires (P=0.0046) under normal conditions (n=60-80 embryos per classification). (D) Embryos produced by high performing sires under normal conditions had significantly higher cleavage rates (P=0.015) than embryos produced by low performing sires under heat stress conditions (n=37 *in vitro* fertilization replicates). (E) There was no difference in blastocyst rate observed between embryos of any group (P>0.05) (n=17 *in vitro* fertilization replicates).

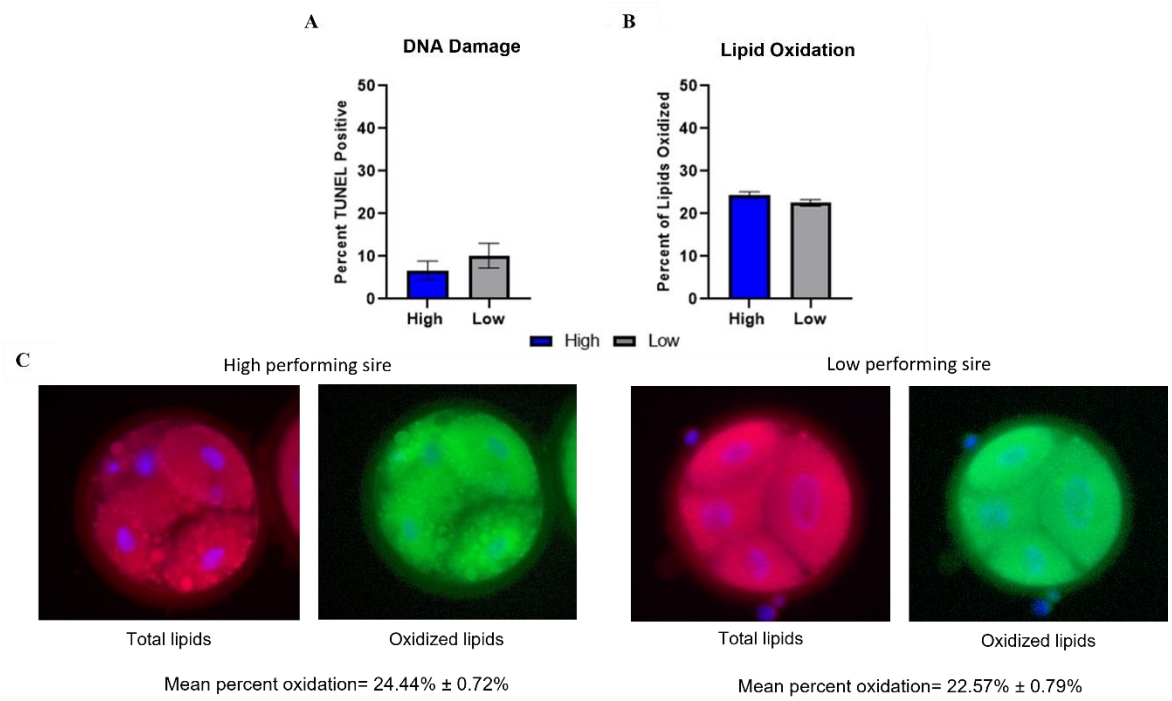

Figure 2.5. DNA damage and percent of lipid oxidation in 2-6 embryos. (A) No significant difference was observed (*P*=0.334) in the percent of TUNEL positive cells in embryos produced by high and low performing sires (n=108-135 embryos per classification). (B) No difference was observed (*P*= 0.079) in the percent of oxidized lipids in embryos produced by high and low performing sires (n=105-130 embryos per classification). (C) Representative images of 2-6 cell embryos produced by high performing sires (left) and low performing sires (right), stained for the quantification of oxidized lipids.

Lipid oxidation

The percentage of lipids oxidized in embryos produced from either high or low performing sires is shown in Figure 2.5B. There was no difference (*P*=0.079) in the percent of lipids that had been oxidized in embryos produced from high performing sires (24.44% ± 0.71%) when compared to embryos produced from low performing sires (22.57% ± 0.79%).

Discussion

There was no difference found in the fertilization rate between groups of sires, which shows that sires with varying fertility status in this study all have an equal ability to effectively penetrate the zona pellucida of an oocyte. Although, differences in cleavage and blastocyst rates indicate that sires do vary in their ability to produce viable embryos that will develop to the blastocyst stage. Following penetration of the zona pellucida, the spermatozoon causes oocyte activation and begins undergoing changes in the oocyte cytoplasm that are crucial for subsequent embryo success. First, the reduction of disulfide bonds between protamine proteins that were incorporated into the sperm's nucleosomes during maturation in the epididymis (Collas & Poccia, 1998; Senger, 2003) and the replacement of protamine proteins by oocyte-derived histones—initially by the linker H1FOO histone (Gao et al., 2004). This parallels the release of the proximal centriole from the spermatozoon, which will recruit maternal pericentriolar material to form a sperm aster. The sperm aster is responsible for bringing the maternal and paternal pronuclei together to allow for pronuclear apposition, which is critical for the formation of the mitotic spindle and the first zygotic cleavage (Avidor-Reiss et al., 2020). Alterations to any of these processes would prevent the first cleavage division and result in arrest. This could explain, in part, why the sire exerts greatest influence on pregnancy success during fertilization and early embryo development.

Embryos produced by low performing sires appear to begin development with an increased level of cellular stress under normal culture conditions— demonstrated by an increase in ROS production as early as the 2-6 cell stage of development. Additionally, 2-6 cell embryos produced by low performing sires had an increased incidence of autophagy. Previous studies have demonstrated that high levels of intracellular ROS lead

to cellular damage, and in embryos, may lead to impaired developmental competence (Sakatani, 2017; Yang et al., 1998). In murine embryos, it was shown that there was an increase in ROS production around the 2 cell stage, which coincided with embryo arrest in that study (Nasr-Esfahani & Johnson, 1991). In the bovine, a reduction in oocytes that developed to the blastocyst stage has been correlated with increased ROS and decreased glutathione levels (Hashimoto et al., 2000).

Under induced stress conditions, in the form of a heat shock, 2-6 cell embryos produced by low performing sires continued to display increased ROS production compared to all other embryos. Alternatively, 2-6 cell heat stressed embryos produced by high performing sires had the highest autophagic activity compared to control embryos produced by either group. Interestingly, there was no difference observed in the autophagic activity in embryos produced by high and low performing sires under control conditions. Although the same sires were used in these experiments, the higher variation in this analysis may be due to an oocyte effect on early embryo development, such as the accumulation of appropriate transcripts to produce proteins necessary for autophagic machinery.

These data show that higher cellular stress leads to an increase in both autophagy and ROS accumulation, with autophagy potentially increasing to mitigate the deleterious impacts of stress. Embryos from low performing sires appear to be unable to upregulate their autophagic pathway to the same capacity that embryos from high sires do, indicating that embryos produced by low performing sires have a less robust mechanism for moderating stress via this pathway. Previous literature has shown that the autophagic pathway is initiated to promote cell survival, such as during cell starvation *in vitro*

(Mizushima, 2007; Song et al., 2012), and has been correlated with embryo development to the blastocyst stage *in vitro* (Balboula et al., 2020; Song et al., 2012).

Although we observed increased ROS production in embryos produced from low performing sires, and it is well documented that ROS may lead to DNA fragmentation (Bayr, 2005; Guerin, 2001), there was no difference found in the DNA damage in embryos from low performing sires in this study. Similarly, there was also no difference found in the oxidation of lipids in embryos from low sires. This leaves us with questions about which pathways are being negatively impacted by increased levels of ROS in early embryos and contributing to lower developmental rates.

Bayr, as well as others, have also shown that ROS overproduction can lead to ER stress and the unfolded protein response in embryonic cells (Bayr, 2005; Yoon et al., 2014). Additionally, it has been demonstrated that the induction of autophagy can alleviate impacts of ER stress in embryos, and inversely, the defects found in autophagy-inhibited embryos can also be alleviated if treated with an ER stress inhibitor as well (Song et al., 2012). Given this data, it is possible that embryos produced by low performing sires may be experiencing ER stress due to their increased ROS production, therefore resulting in the upregulation of autophagic activity to mitigate harmful impacts on embryo development. Further investigation is needed to elucidate how the mechanism of ER stress may be involved in decreased embryo development, and why embryos produced by these low performing sires begin development under high levels of cellular stress.

Chapter 3: The Identification of New Biomarkers of Spermatozoa Quality in Cattle

Introduction

There is currently an outstanding need for the identification of reliable biomarkers of spermatozoa quality in dairy cattle. Until recent years, sperm evaluations during semen processing only included manual assessment of crude morphological features and motility. Although these provide valuable insight into the spermatozoa's ability to reach and fertilize an oocyte, they lack the ability to differentiate which spermatozoa will contribute to a viable embryo past the penetration of the vitelline membrane. Additionally, manual analysis is subjective and lacks standardization across facilities and technicians (Ferrara et al., 1997).

Early embryo mortality is a primary factor contributing to economic loss of the dairy cattle industry, with up to 50% of pregnancy loss occurring within the first seven days following fertilization (Wiltbank et al., 2016). More accurate identification of sire fertility could help to ameliorate this issue, as a sire exhibits a great impact on pregnancy success during fertilization, preimplantation embryo development, conceptus elongation, and placentation (Franco et al., 2020; Ortega et al., 2018; Senger, 2003). No one single bioassay can correctly classify sire fertility, although, a combination of multiple evaluations provides correlation to a sire's ability to successfully produce a viable pregnancy (Attia et al., 2016; Harstine et al., 2018).

In recent years, the use of techniques such as computer assisted sperm analysis (CASA) and flow cytometry have allowed for more accurate quantification of semen

quality (Harstine et al., 2018). The CASA system incorporates videos of sperm microscopy to train computer software programs to evaluate sperm concentration, motility, and morphology (Ferrara et al., 1997). Although this system reduces technician error in manual evaluation, studies with human samples have shown that CASA accuracy decreases with decreased sperm concentrations and therefore fewer cells per field of view (Bar-Chama & Lamb, 1994; Ferrara et al., 1997). Previous literature has described the implementation of flow cytometric analyses with fluorescently labeled sperm cells in human fertility clinics (Da Costa et al., 2021; Ferrara et al., 1997; Perticarari et al., 2007). Using this technology, tens of thousands of sperm cells per sample can be accurately analyzed for a feature of interest in just minutes, which significantly increases the sample size used and decreases variability that is seen in manual evaluation (Perticarari et al., 2007). Flow cytometric sperm analysis is being further elevated by the implementation of machine learning algorithms, used with both fluorescent probes and label-free analyses, in conventional or image-based flow cytometry (Zuidema et al., 2021).

One important marker of sperm quality in live samples is acrosomal integrity, which is commonly assessed via fluorescent labeling using PNA (*Arachis hypogaea*/peanut agglutinin lectin) (Kerns et al., 2018; Rajabi-Toustani et al., n.d.; Sutovsky et al., 2015). Recently, the distribution of zinc (Zn^{2+}) ions present in a spermatozoon has been used to describe stages of sperm capacitation in live samples, and has been associated with varying degrees of fertility (Kerns et al., 2018). This correlation with fertility status may be due to zinc's regulation of the HVCN1 and Catsper proton channels, which are largely responsible for the sperm motility hyperactivation that is achieved following capacitation (Flesch & Gadella, 2000; Kerns et al., 2018).

Additionally, subfertile and infertile bull spermatozoa have been found to exhibit increased ubiquitination which may be contributed by the ubiquitin proteasome system (UPS) in conjunction with protein aggregation during spermatogenesis in the testis and sperm maturation in the epididymis (Cornwall et al., 2011; Sutovsky et al., 2015). Furthermore, the increased ubiquitination of sperm cells has also been correlated with an increase in DNA damage (Sutovsky et al., 2002, 2015). Populations of spermatozoa containing biomarkers such as these can change drastically following a gradient purification protocol, which is performed in preparation for *in vitro* fertilization (IVF). Therefore, it would be beneficial to evaluate spermatozoa both prior to, and following this process to better understand how defective cells can be removed from the sample (Maxwell et al., 2007).

The use of effective biomarkers independent of sire conception rate (SCR) could prove to be most beneficial to the industry due to SCR being determined by confirmed pregnancies at day 70-75 of gestation (Kuhn et al., 2008). A positive SCR value indicates increased fertility, and a negative value indicates decreased fertility. This value is assigned only after AI 300 services have occurred within a four year period, which prevents it's use for younger sires (Norman et al., 2011). Therefore, the identification of biomarkers independent of SCR would allow the biomarkers to be used as a young sire selection tool prior to servicing females.

Previous studies in our laboratory have shown that sires vary in their ability to produce embryos in an *in vitro* culture system, independent of their SCR (Lockhart et al., Submitted JDS 2022; Fallon et al., Chapter 2). Four sires that were high performing at producing embryos and four sires that were low performing at producing embryos, with

varying SCR values, were then selected for subsequent experiments to elucidate mechanisms contributing to this variation. There was no difference observed between groups of sires in their ability to effectively fertilize oocytes and reach the pronuclear stage, although there were differences in developmental competence to the blastocyst stage (Fallon et al., Chapter 2). Embryos at the 2-6 cell stage of development produced by low performing sires exhibited an increase in both ROS production and autophagic activity compared to embryos produced by high performing sires—indicating that these embryos begin development under increased cellular stress (Fallon et al., Chapter 2).

These data make the evaluation of spermatozoa produced by sires of high and low performing classifications an ideal model for identifying new biomarkers of sire fertility, independent of their SCR. This leads to the hypothesis of the current study—that sires with a lower capacity to produce viable blastocysts in an *in vitro* culture system will have spermatozoa that vary from those of sires with a higher capacity to produce embryos. By utilizing this model, it will be possible to identify new characteristics associated with sperm fertility in cattle and elucidate new mechanisms of variation in embryo development caused by sire.

Materials and Methods

Semen preparation

Semen straws used in all experiments were gifted by Select Sires Inc. (Great Plains, OH) and were processed in the same commercial house. Semen was collected from Holstein sires at approximately 28 months of age on average. Four high performing sires and four low performing sires were selected for the experiments of this study based

on previous classification as having high or low capacity to produce embryos (Lockhart et al., submitted JDS; Fallon et al., unpublished). All semen straws were thawed in a water bath at 37° C for 40-45 seconds. Concomitantly, for samples that underwent gradient purification, 600 µl of 50% upper layer isolate gradient was gently pipetted onto 600 µl of 90% lower layer isolate gradient (Irvine Scientific), in a 1.5 ml Eppendorf tube. Semen was extruded from the straw into the isolate tube and centrifuged at 700 g for 5 minutes. The sperm pellet (100 µl) was removed from the bottom of the tube, placed into an Eppendorf tube containing 1ml of warm Hepes-TALP medium, and centrifuged again at 700 g for 5 minutes. This wash step was then repeated once more, for a total of two washes in Hepes-TALP per sample. For samples that did not undergo gradient purification, semen was extruded from the straw directly into 37° C warm Hepes-TALP and washed twice as described above.

DNA damage

DNA integrity was assessed using the In Situ Cell Death Detection Kit (Roche Diagnostics, Ref# 11684809910). Briefly, fixed spermatozoan cells were placed into PBS on poly-L-lysine coated coverslips to adhere for 5 minutes. Cells were subsequently permeabilized for 40 minutes at room temperature (RT) by using PBS with 0.01% Triton X. Following permeabilization, cells were incubated in the manufacturer provided staining solution for 1 hour at 37°C in a humidity chamber shielded from light. Cells were then counterstained with DAPI (1:200) for 15 minutes at RT before being washed for 5 minutes in PBS. Lastly, coverslips were mounted onto glass slides using Vectashield Mounting media (Vector Laboratories, Burlingame, CA, USA) and sealed with clear nail polish. A minimum of 200 cells were analyzed per sample at 40X

magnification and images were recorded with a Nikon Eclipse 800 microscope (Nikon Instruments, Melville, NY, USA) equipped with a Retiga QI-R6 camera (Teledyne QImaging, Surrey, BC, Canada) operated by MetaMorph 7.10.2.240. software (Molecular Devices, San Jose, CA). For all bulls, DNA damage assessments were conducted on both the overall sperm population (pre-gradient) and the gradient separated pellet fraction (post-gradient).

Morphology assessment via immunocytochemistry

Fixed spermatozoa were placed into KMT buffer (100 mM KCl, 2mM $MgCl_2$, 10 mM Tris-HCl, 5mM EGTA, pH 7) on poly-L-lysine coated coverslips to adhere for 20 minutes. Cells were then incubated in a staining solution for 30 minutes at RT shielded from light that contained fluorescent probes that label aggregated proteins (Proteostat Aggresome Detection Kit, ENZ-51035-K100, 1:2,000), the acrosome (PNA-FITC, 1:200) and DNA (DAPI, 1:200), diluted in PBS with 0.01% Triton X. Coverslips were subsequently washed twice, for 5 minutes each with PBS before they were mounted onto glass coverslips using Vectashield Mounting Media (Vector Laboratories, Burlingame, CA, USA) and sealed using clear nail polish. Approximately 110 cells per sample were imaged using differential interference contrast and epifluorescence at 100x magnification. Images were recorded with a Nikon Eclipse 800 microscope (Nikon Instruments, Melville, NY, USA) equipped with a Retiga QI-R6 camera (Teledyne QImaging, Surrey, BC, Canada) operated by MetaMorph 7.10.2.240. software (Molecular Devices, San Jose, CA). Samples were analyzed for morphological features of the acrosome, nucleus, midpiece, principal piece, cytoplasmic droplet retention and aggregated protein contents, and the overall percentage of cells affected by each morphological defect was recorded.

For all bulls, morphological assessments were conducted on both the overall sperm population (pre-gradient) and the gradient separated pellet fraction (post-gradient) used for IVF.

Image-based flow cytometry with fixed samples

Following semen preparation, spermatozoa were fixed in 2% formaldehyde for 20 minutes before being subsequently incubated for 30 minutes in the dark at RT in a staining solution containing an aggresome probe (Proteostat Aggresome Detection Kit, ENZ-51035-K100, 1:10,000), PNA-FITC (1:2500) and the nuclear stain Hoescht33342 (1:1000) diluted in PBS with 0.01% Triton X. Lectin PNA was used to validate that permeabilization was achieved, such that the aggresome probe had the ability to target intracellular protein aggregates. After staining, samples were spun down using centrifugation (700 *x g,* 5 minutes) to remove the staining solution and resuspended in PBS for analysis. Samples were then analyzed with an Amnis FlowSight imaging flow cytometer (EMD Millipore Corp., Seattle, WA, USA) fitted with a 20X microscope objective (numerical aperture of 0.5) with an imaging rate of up to 2,000 events/sec. The sheath fluid was PBS, free of $Ca^{2+}$and Mg^{2+}. The flow-core size was 10 μm diameter and speed was 66 mm/sec, respectively. Raw images were acquired using INSPIRE® software (Amnis-Millipore). The camera was set to 1.0 μm per pixel of the charged-coupled device. The image display dimension for the field of view was 60 μm and 8 μm depth of field. Samples were analyzed using three lasers simultaneously: a 405-nm line with intensity set to 10 mW; a 488-nm line with intensity set to 30 mW; and a 785-nm line (side scatter) with intensity set to 50 mW. A total of 10,000 events were collected per sample. Data analysis of the raw images was performed using the IDEAS® software

(Version 6.2.64.0; Amnis-Millipore), where the electronic images were compensated for channel crossover by using single-color controls that were merged to generate a multi-color matrix. The compensation matrix file was then applied to a raw-image file (.rif), to create a color-compensated image file (.cif). A focused spermatozoa population was created by gating cells using Gradient RMS for the bright field channel. Single-cell events were gated by combining the Area × Aspect Ratio scatter plot of the brightfield, from the first step, with that of the DAPI channel. A single cell population gate was used for the histogram display of mean pixel intensities by frequency for the following channels: FITC (channel 2), DAPI (channel 7), and TRITC (channel 3). Intensity histograms for the individual channels were then used to gate sub-populations with varying intensity levels and visual conformations. All analyses of aggresome content (sperm head only and total) were gated from 683-10625.

Image-based flow cytometry with live samples

Following semen preparation, approximately 5 million gradient purified spermatozoa were resuspended in HEPES-buffered Tyrode lactate medium supplemented with polyvinyl alcohol (TL-HEPES-PVA), containing 10 mM sodium lactate, 5.2 mM sodium pyruvate, 11 mM D-glucose, 0.5 mM $MgCl_2$ and 0.01% (w/v) polyvinyl alcohol (PVA), and void of Ca^{2+} and HCO_3^- ions; pH = 7.2, t = 37°C. The following probe combinations were added to the sperm suspension to the final concentrations: 1) FluoZin-3, AM (1 µM), H33342 (18 µM), Propidium Iodide (PI, 1 $\mu g \cdot mL^{-1}$), and peanut agglutinin conjugated to AF647 (PNA-AF647, 0.5 $\mu g \cdot mL^{-1}$), or ii) FluoZin-3, AM (1 µM), H33342 (18 µM), Propidium Iodide (PI, 1 $\mu g \cdot mL^{-1}$), CellROX™ Deep Red (10µM). Sperm samples were left to incubate for 40 minutes at 37°C in the dark.

The fluorescently labeled samples were measured with an Amnis FlowSight Imaging Flow Cytometer (AMNIS Luminex Corporation, Austin, TX) as described previously (Kennedy et al., 2014; Kerns et al., 2018). The instrument was fitted with a 20X microscope objective (numerical aperture of 0.9) with an imaging rate of up to 2,000 events per sec. The sheath fluid was PBS (without Ca^{2+} or Mg^{2+}). The flow-core diameter and speed were 10 µm and 66 mm per second, respectively. The raw image data were acquired using INSPIRE® software (AMNIS Luminex Corporation, Austin, TX). To produce the highest resolution, the camera setting was at 1.0 µm per pixel of the charge-coupled device. Samples were analyzed using four lasers concomitantly: a 405-nm line (20 mW), 488-nm line (60 mW), 642-nm line (75 mW) a 785-nm line (70 mW, side scatter), and two LEDs (32.57 mW and 19.30 mW respectively). Signals were observed in the following channels: channels 1 and 9 - brightfield, channel 2 – green fluorescence (FZ3, 505-560 nm), channel 6 (SSC), channel 7 – blue fluorescence (H33342, 435-505 nm), and channel 11 – infrared fluorescence (AF647, DeepRed; 642-745 nm;). A total of 10,000 events were collected per sample, and data were analyzed using IDEAS® software (Version 6.2.64.0; AMNIS Luminex Corporation, Austin, TX). A focused, single-cell population gate with anteriorly/posteriorly oriented spermatozoa (Kerns et al., 2018) was used for histogram display of mean pixel intensities by frequency for collected channels. Intensity histograms of individual channels were then used for drawing regions of subpopulations with varying intensity levels and visual confirmation. The intensity of H33342 was used for histogram normalization among samples.

Results

DNA damage

The DNA damage present in spermatozoa from either high or low performing sires is shown in Figure 3.1. The percent of TUNEL positive sperm cells in samples prior to gradient purification was significantly increased (P<0.0001) in samples from low performing sires (28.85% ± 1.37) compared to those from high performing sires (17.67% ± 1.09%). Conversely, the percent of TUNEL positive sperm cells in samples following gradient purification was significantly increased (P<0.0001) in samples from high performing sires (12.44% ± 0.95%) compared to those from low performing sires (5.95% ± 0.71%).

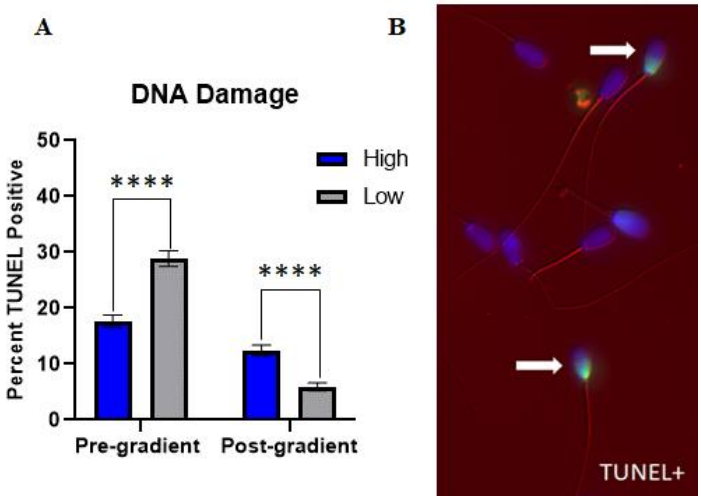

Figure 3.1. Sperm DNA damage. (A) In samples prior to gradient purification, termed pre-gradient samples, there was an increase in DNA damage present (P<0.0001) in spermatozoa from low performing sires compared to high performing. Inversely, in samples following gradient purification, termed post-gradient samples, there was an increase in DNA damage present (P<0.0001) in high performing sires compared to low performing (n= ~1,000 cells per classification). (B) Representative image of TUNEL negative and TUNEL positive spermatozoa.

Morphology assessment via immunocytochemistry

The following morphological features were evaluated to investigate the presence of defects, using immunocytochemistry and fluorescent microscopy: acrosome structure, nucleus, aggresome content, tail midpiece structure, and tail principal piece morphology

(Figure 3.2). In pre-gradient samples, there was no difference observed in acrosome defects (P=0.978) between high performing (15.88% ± 1.69%) and low performing sires (15.94% ± 1.62%). There was also no difference in nuclear defects (P=0.284) or midpiece defects (P=0.601) between high performing (18.88% ±1.81%; 14.16% ±1.62%) and low performing sires (21.65% ± 1.83%; 15.35% ± 1.60%). In pre-gradient samples, low performing sires had an increased incidence of aggresome defects in the head of the spermatozoa (P=0.0001; 24.41% ± 1.91%) compared to high performing sires (14.38% ± 1.63%). Alternatively, high performing sires had increased total tail defects (P<0.0001; 34.98% ± 2.20%) when compared to low performing sires (21.06% ± 1.81%). In post-gradient samples, there were no differences in acrosome defects (P=0.795) or nuclear defects (P=0.132) between high performing (6.98% ± 1.21%; 11.04% ± 1.49%) and low performing sires (7.43% ± 1.24%; 14.41% ± 1.67%). Similarly, there were no differences in aggresome defects (P=0.390) or midpiece defects (P=0.401) between high performing (4.5% ± 0.98%; 6.76% ± 1.12%) and low performing sires (3.38% ± 0.86%; 5.41% ± 1.07%). Finally, in post-gradient samples, there was also no difference in total tail defects (P=0.623) between high performing (13.96% ± 1.65%) and low performing sires (12.84% ± 1.59%).

Image-based flow cytometry on fixed samples

To quantify the aggresome content in spermatozoa from high and low performing sires, fixed samples were stained and analyzed using image-based flow cytometry. These data are shown in Figure 3.3 and the supplementary information. In samples prior to gradient purification, there was no difference (P=0.818) between the aggresome content in the sperm heads from low performing sires (58.53% ± 8.53%) compared to high

performing sires (55.53% ± 8.53%). Additionally, there was no difference (*P*=0.132) between the total aggresome content in sperm cells from low performing sires (94.42% ± 1.47%) compared to high performing sires (97.71% ± 1.47%; Supplementary Figure 1A). In samples following gradient purification, sperm cells from low performing sires had significantly increased incidence (*P*=0.032) of aggresome content in their heads (55.78% ± 7.24%) compared to sperm cells from high performing sires (28.68% ± 9.23%). Alternatively, there was again no difference (*P*=0.217) between total aggresome content in sperm cells from low sires (90.4% ± 2.39%) compared to high sires (95.35% ± 3.05%; Supplementary Figure 1B), which indicates consistent labeling in the tail midpiece.

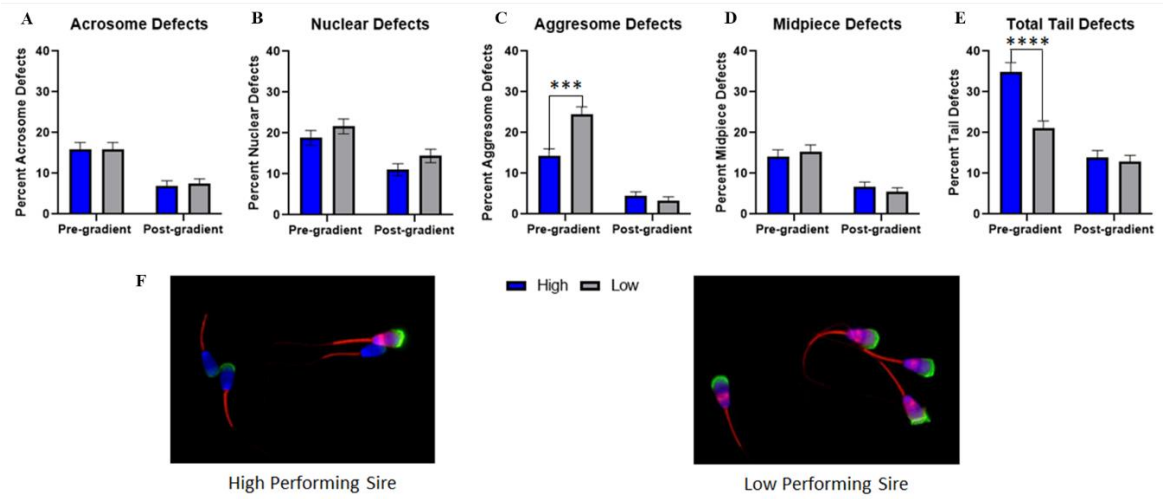

Figure 3.2. Morphological assessment via immunocytochemistry. (A) In samples prior to gradient purification, termed pre-gradient samples, there was no difference (*P*=0.978) in acrosome defects between high and low performing sires. In samples following gradient purification, termed post-gradient samples, there was also no difference (*P*=0.795) in acrosome defects between high and low sires. (B) In both pre-gradient and post-gradient samples, there were no differences in nuclear defects (*P*=0.284; *P*=0.132) between high and low performing sires. (C) In pre-gradient samples, low performing sires had a significantly higher incidence of aggresome defects in the head (*P*=0.0001) compared to high performing sires. In post-gradient samples, there was no difference observed between high and low sires (*P*=0.390). (D) In both pre-gradient and post-gradient samples, there were no differences in midpiece defects (*P*=0.601; *P*=0.401) between high and low performing sires. (E) In pre-gradient samples, high performing sires had a significantly higher incidence of tail defects (*P*<0.0001) compared to low performing sires. In post-gradient samples, there was no difference observed between high and low sires (*P*=0.623) (n= ~450 cells per classification for all evaluations). (F) Representative images of fluorescently labeled spermatozoa from a high performing sire (left) and a low performing sire (right).

Image-based flow cytometry on live samples

To evaluate the viability of live spermatozoa following gradient purification, sperm cells were co-stained with zinc ion, viability and ROS probes and analyzed using image-based flow cytometry. These data are shown in Figure 3.4. The populations of spermatozoa in these samples segregated as follows: Population 1 (zinc labeling in the whole head + midpiece + some principal piece, PI-, ROS+), Population 2 (zinc labeling in the acrosome + midpiece, PI+, ROS-), Population 3 (zinc labeling in the midpiece only, PI+, ROS-), and Population 4 (no zinc labeling, PI+, ROS-). In the high performing sires, there was a significantly higher percentage of population 1 (33.48% ± 8.91%; P=0.024) and population 3 (39.63% ± 8.91%; P=0.008) when compared to population 4 (3.17% ± 8.91%). In the low performing sires, there was a significantly higher percentage of population 3 (53.95% ± 8.91%) than all others: population 1 (9.15% ± 8.91%; P=0.002), population 2 (25.22% ± 8.91%; P= 0.032), and population 4 (4.7% ± 8.91%; P=0.0007).

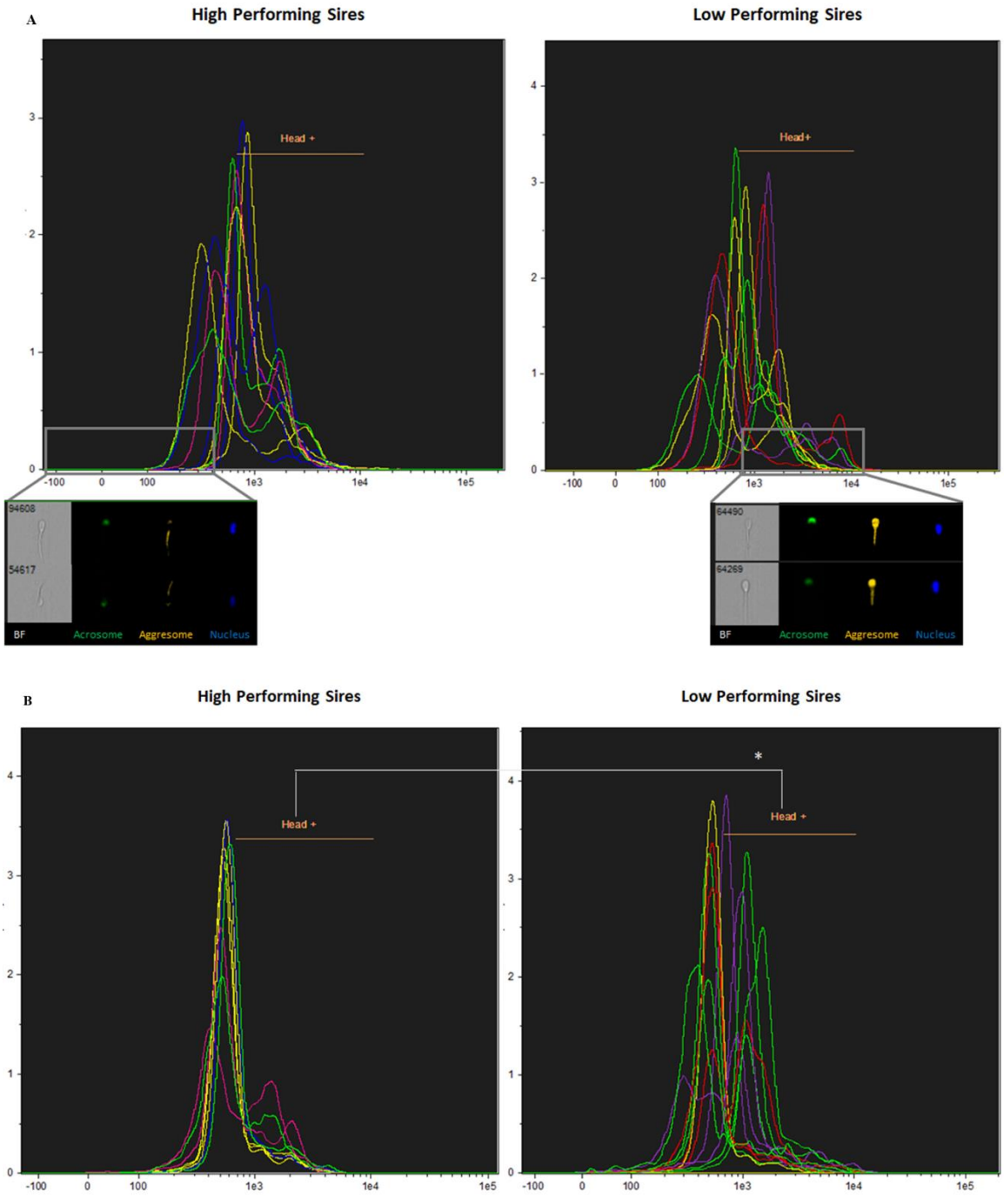

Figure 3.3. Quantification of aggresome defects in heads of spermatozoa. (A) In pre-gradient samples, there was no difference in the percent of spermatozoa with aggresome defects in the head (*P*=0.818) between high and low performing sires. (B) In post-gradient samples, low performing sires had a significantly higher incidence of aggresome defects in the head (P=0.03) compared to high performing (n= ~90,000 cells per classification).

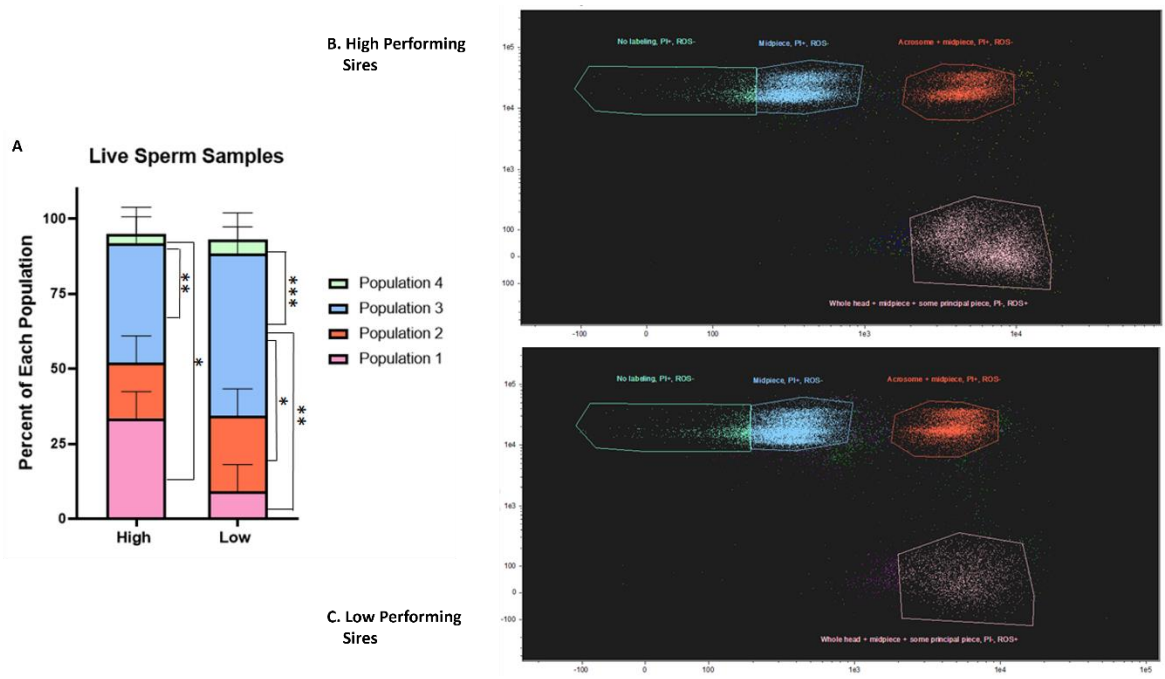

Figure 3.4. Quantification of spermatozoa viability and capacitation status in live, post-gradient samples. (A) Differences in populations of live, post-gradient samples (n= ~35,000 cells per classification) ranging from live, non-capacitated (Population 1) to moribund, post -capacitated spermatozoa (Population 4). Population 1= zinc labeling in the whole head + midpiece + proximal principal piece, PI-, ROS+, Population 2= zinc labeling in the acrosome + midpiece, PI+, ROS-, Population 3= zinc labeling in the midpiece only, PI+, ROS-, and Population 4= no zinc labeling, PI+, ROS-. In high performing sires, there was a significantly higher percentage of Population 1 (P=0.024), and Population 3 (P=0.008) when compared to Population 4. In low performing sires, there was a higher percentage of Population 3 that all others: Population 1 (P=0.002), Population 2 (P=0.032), and Population 4 (P=0.0007). (B) Scatterplot showing the segregation of populations in high performing sires. (C) Scatterplot showing the segregation of populations in low performing sires.

Discussion

This study evaluated spermatozoa from samples, both prior to and following gradient purification, to validate candidate biomarkers of sire fertility and to understand how the presence of those biomarkers may be impacted by gradient purification. It has been documented in many species that utilizing a density gradient combined with centrifugation will increase the percentage of motile, morphologically normal sperm cells

in a given sample (Eberhardt et al., 2022; Maxwell et al., 2007; Phillips et al., 2012). Although, this also reduces the number of total cells that remain following the process. Spermatozoa from pre-gradient samples of low performing sires had increased DNA damage, but in post-gradient samples, the inverse was observed, and high performing sires had increased DNA damage. Gradient purification would have the most substantial impact on removing spermatozoa with DNA damage when those cells were also compromised with other defects, or already dead (Ahlering et al., 2020; Tomlinson et al., 2001). If a greater percentage of DNA-damaged spermatozoa from low performing sires were dead upon thawing the semen straws, there would be a greater number of cells removed from the post-gradient population, which was observed in this study. This could explain why there was more DNA damage remaining in the post-gradient samples from high performing sires, particularly if there is a discrete cohort of live, motile spermatozoa with DNA damage in bull semen (Dogan et al., 2015).

It is unexpected to label aggresomes in the heads of viable spermatozoa, although consistent labeling in the head was seen in some samples during the immunocytochemistry evaluation of this study. In pre-gradient samples, the most prevalent defect identified in low performing sires was the increased aggresome content in the head, specifically located in the post-acrosomal sheath region. Conversely, the most prevalent defects identified in the high performing sires were in the tail, which are commonly removed with gradient purification because of their impaired motility (Maxwell et al., 2007; Morrell et al., 2009; Phillips et al., 2012). This may partially explain the discrepancy of why some sires produce increased numbers of viable embryos

in vitro, following a gradient purification protocol but had lower SCR values when used to service females *in vivo*.

The use of image-based flow cytometry to quantify aggresome content in the heads of spermatozoa allowed for a much larger sample size to be evaluated—approximately 90,000 cells per sire classification. In post-gradient samples, low performing sires had an increased incidence of aggresome defects in the head compared to high performing sires. The large sample size that was evaluated could explain the difference in results from the immunocytochemistry assessment and indicate more robust results using flow cytometry. From the pre-gradient to the post-gradient samples, high performing sires had a 30% reduction in cells containing this defect, indicating that many positive cells were removed during gradient purification. This resulted in less variation between post-gradient samples from the high performing sires. Samples from low performing sires had a mere 3% reduction in cells containing this defect from the pre to the post-gradient evaluation, indicating that this defect alone is less impacted by gradient purification.

When unfolded or misfolded proteins are not corrected or degraded rapidly enough, it allows other proteins the chance to interact with them, sometimes leading to the formation of large protein aggregates (Garcia-Mata et al., 2002). Aggresomes have the potential to form in any cell type, are associated with cell death, and have been linked to neurodegenerative diseases such as Alzheimer's and Huntington's disease, as well as systemic amyloidosis (Garcia-Mata et al., 2002; Kopito, 2000). Once aggresomes form in a cell, they need to be cleared via autophagic degradation before continuing to promote further aggregate enlargement (Driscoll & Chowdhury, 2012; Garcia-Mata et al., 2002).

If degradation fails to occur efficiently, cellular proteostasis becomes perturbed—leading to cell damage and potentially apoptosis. In the mouse, a cysteine protease inhibitor, cystatin-related epididymal spermatogenic (CRES), has been found to self-aggregate *in vitro*, forming amyloid-like aggresomes (Cornwall et al., 2011). Additionally, CRES is secreted by the initial segment of the epididymis, with the potential to form aggresomes in the epididymal lumen, and commonly present in the sperm acrosome (Cornwall et al., 2011).

In the evaluation of live spermatozoa following gradient purification, four distinct populations were identified in the samples, with Population 1 being the most viable and Population 4 being the least viable. Interpretation of zinc labeling was based off previous literature by Kerns et al (2018). Population 1 was composed of spermatozoa that had not begun sperm capacitation associated with zinc efflux, had no plasma membrane alteration indicated by PI labeling, and had a presence of ROS. Population 2 was composed of spermatozoa in early-stage capacitation, had membrane alteration, and had less ROS—indicating ROS consumption and possibly less mitochondrial activity. Population 3 was composed of spermatozoa in late-stage capacitation, had membrane alteration, and had less ROS—indicating ROS consumption and possibly less mitochondrial activity. Finally, Population 4 was composed of spermatozoa that were fully capacitated or dead, had membrane alteration, and had no ROS present. The high performing sires had significantly more viable sperm cells, in Population 1, than non-viable sperm cells, in Population 4. The largest proportion of sperm cells from low performing sires were in Population 3 and were therefore less viable. These data suggest that there is a further reduction in the number of spermatozoa produced by low performing sires following

gradient purification, due to a large proportion of less viable cells that may be unable to successfully contribute to embryo development.

Although previous studies in our lab have shown that there was no difference between groups of sires with varied SCR values in their ability to effectively fertilize oocytes and reach the pronuclear stage, there were differences in developmental competence and cellular stress indicators observed in the subsequent embryos (Fallon et al., Chapter 2). If the number of spermatozoa from low performing sires that can reach and fertilize an oocyte have been reduced due to gradient purification and a higher proportion of less viable cells, then the population that reaches the oocyte may be enriched for defects such as aggresomes located in their heads. Upon incorporation into the fertilized oocyte, aggresomes may overwhelm protein degradation machinery in the zygote—potentially leading to the upregulation in autophagic activity and ROS production that was observed in early embryos produced by low performing sires (Fallon et al., Chapter 2). This indicates that it may prove to be beneficial to evaluate semen separately for AI use *in vivo* vs. *in vitro* embryo production.

One previous study has also identified increased protein aggregates in defective spermatozoa (Kennedy et al., 2014). Additionally, it has been shown that not all types of aggresomes are equally cleared via the autophagic pathway in neuroblastoma cells, indicating that there is selectivity to this relationship and that some cells may be more susceptible to slower degradation than others (Wong et al., 2008). Furthermore, dense protein aggregates being located in the post-acrosomal sheath region could potentially impair the release of the SOAF, therefore impacting oocyte activation at fertilization (Kennedy et al., 2014). The identification of this phenomenon could explain the

malfunction of one cellular mechanism regulated by sire during early embryo development and serve as a biomarker of spermatozoa quality and sire fertility in the future.

Conclusions

Prior to this study, it was understood that commercial sires differ in their ability to produce blastocysts in an *in vitro* culture system, independent of their SCR, yet our understanding of the malfunction of cellular mechanisms regulated by sire during early embryo development was still lacking. This project worked to elucidate these mechanisms that are influenced by sire—leading to a deeper understanding of early embryo mortality, as well as the identification of new fertility-related biomarkers of spermatozoa.

We demonstrated that although there is no difference in the IVF fertilization rate of our high and low performing sires, there is a difference in developmental competence to the blastocyst stage. Additionally, embryos produced by low performing sires have an upregulation of cellular stress indicators: ROS production and autophagy, at the 2-6 cell stage of development. Which downstream mechanisms may be impacted by increased ROS production is still unknown, as neither DNA damage nor lipid oxidation were increased in embryos produced by low performing sires. It is hypothesized that embryos produced by low performing sires may be experiencing ER stress due to their increased ROS production, therefore resulting in the upregulation of autophagic activity to mitigate harmful impacts on embryo development. Further investigation is needed to elucidate how the mechanism of ER stress may be involved in decreased embryo development.

Upon investigating characteristics of spermatozoa from high and low performing sires, a few key differences were identified. Using image-based flow cytometry, it was observed that following gradient purification, spermatozoa from low performing sires had an increase in aggresome defects in their heads, as well as a greater proportion of cells that underwent premature capacitation, had membrane alteration, and had lack of ROS production, indicating lesser mitochondrial activity. If the number of spermatozoa from low performing sires that can reach and fertilize an oocyte have been reduced due to gradient purification and a higher proportion of less viable cells, then the population that reaches the oocyte may be enriched for defects such as aggresomes located in their heads. At the time of fertilization, the aggresomes may be incorporated into the fertilized oocyte—potentially impairing oocyte activation and overwhelming protein degradation machinery in the zygote, such as autophagic machinery, and leading to high levels of cellular stress. The identification of this phenomenon could explain the malfunction of one cellular mechanism regulated by sire during early embryo development and serve as a biomarker of spermatozoa quality and sire fertility in the future.

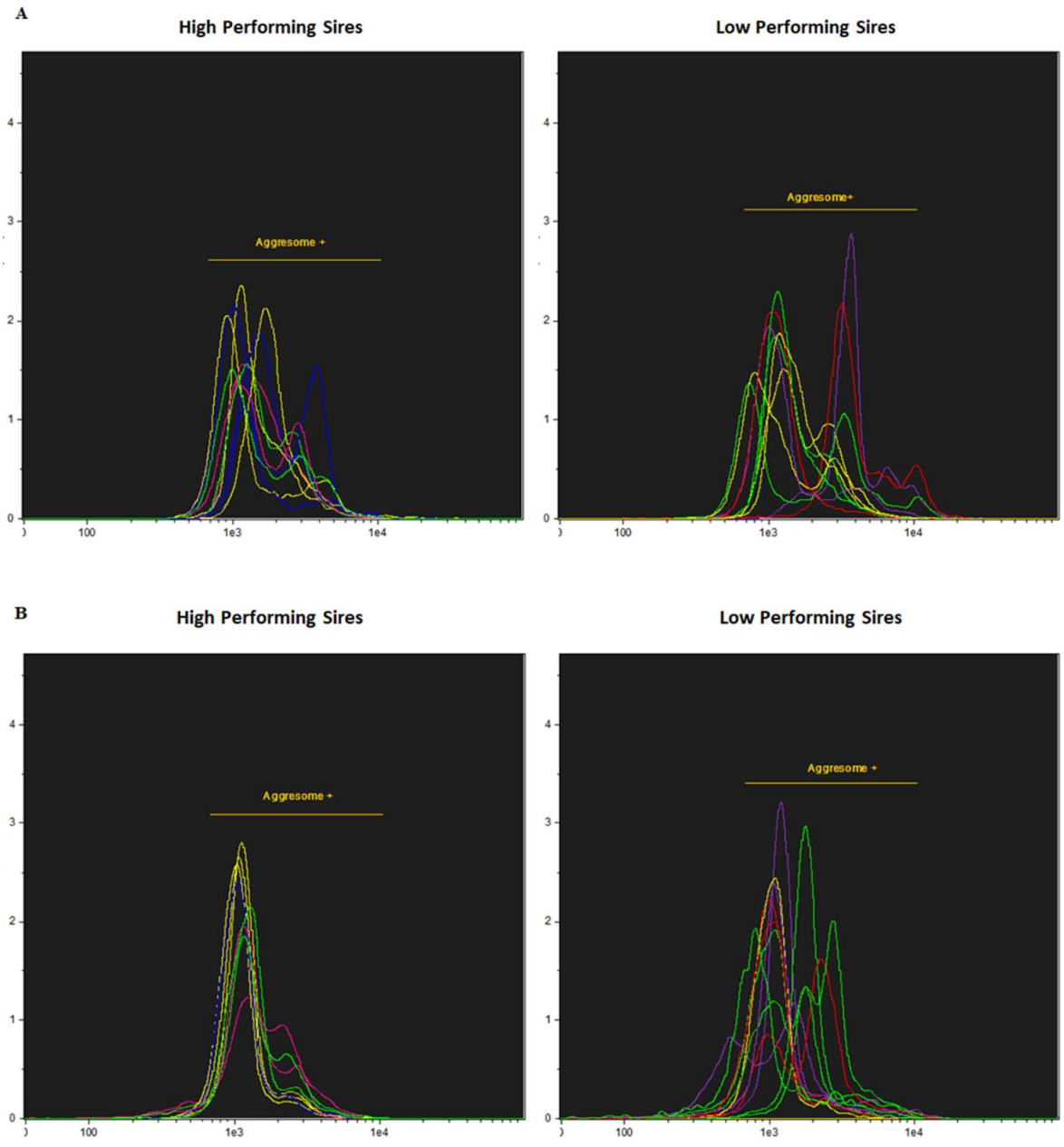

Figure S1. Total sperm aggresome content. (A) In pre-gradient samples, there was no difference in total aggresome content (P=0.132) of high and low performing sires. (B) In post-gradient samples, there was no difference in total aggresome content (P=0.217) of high and low performing sires, most likely due to signal contributed by tail midpiece.

References

Ahlering, P., Sutovsky, M., Gliedt, D., Branson, K., Miranda Vizuete, A., & Sutovsky, P. (2020). Sperm content of TXNDC8 reflects sperm chromatin structure, pregnancy establishment, and incidence of multiple births after ART. *Systems Biology in Reproductive Medicine*, *66*(5), 311–321. https://doi.org/10.1080/19396368.2020.1801889

Al-Katanani, Y. M., & Hansen, P. J. (2002). Induced thermotolerance in bovine two-cell embryos and the role of heat shock protein 70 in embryonic development. *Molecular Reproduction and Development*, *62*(2), 174–180. https://doi.org/10.1002/mrd.10122

Arand, J., Reijo Pera, R. A., & Wossidlo, M. (2021). Reprogramming of DNA methylation is linked to successful human preimplantation development. *Histochemistry and Cell Biology*, *156*(3), 197–207. https://doi.org/10.1007/s00418-021-02008-6

Attia, S., Katila, T., & Andersson, M. (2016). The Effect of Sperm Morphology and Sire Fertility on Calving Rate of Finnish Ayrshire AI Bulls. *Reproduction in Domestic Animals*, *51*(1), 54–58. https://doi.org/10.1111/rda.12645

Avidor-Reiss, T., Carr, A., & Fishman, E. L. (2020). The sperm centrioles. *Molecular and Cellular Endocrinology*, *518*, 110987. https://doi.org/10.1016/j.mce.2020.110987

Balboula, A. Z., Aboelenain, M., Li, J., Bai, H., Kawahara, M., Abdel-Ghani, M. A., & Takahashi, M. (2020). Inverse relationship between autophagy and CTSK is

related to bovine embryo quality. *Reproduction*, *159*(6), 757–766. https://doi.org/10.1530/REP-20-0036

Banhegyi, G., Baumeister, P., Benedetti, A., Dong, D., Fu, Y., Lee, A. S., Li, J., Mao, C., Margittai, E., Ni, M., Paschen, W., Piccirella, S., Senesi, S., Sitia, R., Wang, M., & Yang, W. (2007). Endoplasmic Reticulum Stress. *Annals of the New York Academy of Sciences*, *1113*(1), 58–71. https://doi.org/10.1196/annals.1391.007

Bar-Chama, N., & Lamb, D. J. (1994). EVALUATION OF SPERM FUNCTION: What Is Available in the Modern Andrology Laboratory? *Urologic Clinics of North America*, *21*(3), 433–446. https://doi.org/10.1016/S0094-0143(21)00618-2

Barcroft, L. C., Offenberg, H., Thomsen, P., & Watson, A. J. (2003). Aquaporin proteins in murine trophectoderm mediate transepithelial water movements during cavitation. *Developmental Biology*, *256*(2), 342–354. https://doi.org/10.1016/S0012-1606(02)00127-6

Barth, A.D. & Oko, R.J. (1989). *Abnormal Morphology of Bovine Spermatozoa* (1st ed.). Iowa State University Press.

Bayr, H. (2005). Reactive oxygen species: *Critical Care Medicine*, *33*(Suppl), S498–S501. https://doi.org/10.1097/01.CCM.0000186787.64500.12

Benammar, A., Ziyyat, A., Lefèvre, B., & Wolf, J.-P. (2017). Tetraspanins and Mouse Oocyte Microvilli Related to Fertilizing Ability. *Reproductive Sciences*, *24*(7), 1062–1069. https://doi.org/10.1177/1933719116678688

Bianchi, E., Doe, B., Goulding, D., & Wright, G. J. (2014). Juno is the egg Izumo receptor and is essential for mammalian fertilization. *Nature*, *508*(7497), 483–487. https://doi.org/10.1038/nature13203

Bultman, S. J., Gebuhr, T. C., Pan, H., Svoboda, P., Schultz, R. M., & Magnuson, T. (2006). Maternal BRG1 regulates zygotic genome activation in the mouse. *Genes & Development*, *20*(13), 1744–1754. https://doi.org/10.1101/gad.1435106

Campbell, K. D., Reed, W. A., & White, K. L. (2000). Ability of Integrins to Mediate Fertilization, Intracellular Calcium Release, and Parthenogenetic Development in Bovine Oocytes1. *Biology of Reproduction*, *62*(6), 1702–1709. https://doi.org/10.1095/biolreprod62.6.1702

Cavallari, F. de C., Leal, C. L. V., Zvi, R., & Hansen, P. J. (2019). Effects of melatonin on production of reactive oxygen species and developmental competence of bovine oocytes exposed to heat shock and oxidative stress during *in vitro* maturation. *Zygote*, *27*(3), 180–186. https://doi.org/10.1017/S0967199419000236

Cecconi, F., & Levine, B. (2008). The Role of Autophagy in Mammalian Development: Cell Makeover Rather than Cell Death. *Developmental Cell*, *15*(3), 344–357. https://doi.org/10.1016/j.devcel.2008.08.012

Cerri, R. L. A., Rutigliano, H. M., Chebel, R. C., & Santos, J. E. P. (2009). Period of dominance of the ovulatory follicle influences embryo quality in lactating dairy cows. *Reproduction*, *137*(5), 813–823. https://doi.org/10.1530/REP-08-0242

Chan, L. L.-Y., Shen, D., Wilkinson, A. R., Patton, W., Lai, N., Chan, E., Kuksin, D., Lin, B., & Qiu, J. (2012). A novel image-based cytometry method for autophagy detection in living cells. *Autophagy*, *8*(9), 1371–1382. https://doi.org/10.4161/auto.21028

Chenoweth, P. J. (2005). Genetic sperm defects. *Theriogenology*, *64*(3), 457–468. https://doi.org/10.1016/j.theriogenology.2005.05.005

Citi, S. (1993). The molecular organization of tight junctions. *Journal of Cell Biology*, *121*(3), 485–489. https://doi.org/10.1083/jcb.121.3.485

Collas, P., & Poccia, D. (1998). Remodeling the sperm nucleus into a male pronucleus at fertilization. *Theriogenology*, *49*(1), 67–81. https://doi.org/10.1016/S0093-691X(97)00403-2

Cornwall, G. A., von Horsten, H. H., & Whelly, S. (2011). Cystatin-Related Epididymal Spermatogenic Aggregates in the Epididymis. *Journal of Andrology*, *32*(6), 679–685. edswsc. https://doi.org/10.2164/jandrol.111.012963

Da Costa, R., Redmann, K., & Schlatt, S. (2021). Simultaneous detection of sperm membrane integrity and DNA fragmentation by flow cytometry: A novel and rapid tool for sperm analysis. *Andrology*, *9*(4), 1254–1263. https://doi.org/10.1111/andr.13017

de Castro e Paula, L. A., & Hansen, P. J. (2008). Modification of actions of heat shock on development and apoptosis of cultured preimplantation bovine embryos by oxygen concentration and dithiothreitol. *Molecular Reproduction and Development*, *75*(8), 1338–1350. https://doi.org/10.1002/mrd.20866

Diskin, M., & Morris, D. (2008). Embryonic and Early Foetal Losses in Cattle and Other Ruminants. *Reproduction in Domestic Animals*, *43*(s2), 260–267. https://doi.org/10.1111/j.1439-0531.2008.01171.x

Dogan, S., Vargovic, P., Oliveira, R., Belser, L. E., Kaya, A., Moura, A., Sutovsky, P., Parrish, J., Topper, E., & Memili, E. (2015). Sperm Protamine-Status Correlates to the Fertility of Breeding Bulls1. *Biology of Reproduction*, *92*(4). https://doi.org/10.1095/biolreprod.114.124255

Driscoll, J. J., & Chowdhury, R. D. (2012). Molecular crosstalk between the proteasome, aggresomes and autophagy: Translational potential and clinical implications. *Cancer Letters*, *325*(2), 147–154. https://doi.org/10.1016/j.canlet.2012.06.016

Eberhardt, M., Prochowska, S., Duszewska, A. M., Van Soom, A., Olech, W., & Niżański, W. (2022). The influence of Percoll® density gradient centrifugation before cryopreservation on the quality of frozen wisent (Bison bonasus) epididymal spermatozoa. *BMC Veterinary Research*, *18*(1), 305. https://doi.org/10.1186/s12917-022-03408-z

Ferrara, F., Daverio, R., Mazzini, G., Bonini, P., & Banfi, G. (1997). Automation of human sperm cell analysis by flow cytometry. *Clinical Chemistry*, *43*(5), 801–807. https://doi.org/10.1093/clinchem/43.5.801

Flesch, F. M., & Gadella, B. M. (2000). Dynamics of the mammalian sperm plasma membrane in the process of fertilization. *Biochimica et Biophysica Acta (BBA) - Reviews on Biomembranes*, *1469*(3), 197–235. https://doi.org/10.1016/S0304-4157(00)00018-6

Franco, G., Reese, S., Poole, R., Rhinehart, J., Thompson, K., Cooke, R., & Pohler, K. (2020). Sire contribution to pregnancy loss in different periods of embryonic and fetal development of beef cows. *Theriogenology*, *154*, 84–91. https://doi.org/10.1016/j.theriogenology.2020.05.021

Gahlay, G., Gauthier, L., Baibakov, B., Epifano, O., & Dean, J. (2010). Gamete Recognition in Mice Depends on the Cleavage Status of an Egg's Zona Pellucida Protein. *Science*, *329*(5988), 216–219. https://doi.org/10.1126/science.1188178

Gao, S., Chung, Y. G., Parseghian, M. H., King, G. J., Adashi, E. Y., & Latham, K. E. (2004). Rapid H1 linker histone transitions following fertilization or somatic cell nuclear transfer: Evidence for a uniform developmental program in mice. *Developmental Biology*, *266*(1), 62–75. https://doi.org/10.1016/j.ydbio.2003.10.003

Garcia-Mata, R., Gao, Y.-S., & Sztul, E. (2002). Hassles with Taking Out the Garbage: Aggravating Aggresomes: Aggresomal Pathway for Protein Degradation. *Traffic*, *3*(6), 388–396. https://doi.org/10.1034/j.1600-0854.2002.30602.x

Gatimel, N., Moreau, J., Parinaud, J., & Léandri, R. D. (2017). Sperm morphology: Assessment, pathophysiology, clinical relevance, and state of the art in 2017. *Andrology*, *5*(5), 845–862. https://doi.org/10.1111/andr.12389

Graf, A., Krebs, S., Zakhartchenko, V., Schwalb, B., Blum, H., & Wolf, E. (2014). Fine mapping of genome activation in bovine embryos by RNA sequencing. *Proceedings of the National Academy of Sciences*, *111*(11), 4139–4144. https://doi.org/10.1073/pnas.1321569111

Guerin, P. (2001). Oxidative stress and protection against reactive oxygen species in the pre-implantation embryo and its surroundings. *Human Reproduction Update*, *7*(2), 175–189. https://doi.org/10.1093/humupd/7.2.175

Gupta, S. K. (2021). Human Zona Pellucida Glycoproteins: Binding Characteristics with Human Spermatozoa and Induction of Acrosome Reaction. *Frontiers in Cell and Developmental Biology*, *9*, 619868. https://doi.org/10.3389/fcell.2021.619868

Hamze, J. G., Sánchez, J. M., O'Callaghan, E., McDonald, M., Bermejo-Álvarez, P., Romar, R., Lonergan, P., & Jiménez-Movilla, M. (2020). JUNO protein coated

beads: A potential tool to predict bovine sperm fertilizing ability. *Theriogenology*, *155*, 168–175. https://doi.org/10.1016/j.theriogenology.2020.05.025

Harstine, B. R., Utt, M. D., & DeJarnette, J. M. (2018). Review: Integrating a semen quality control program and sire fertility at a large artificial insemination organization. *Animal*, *12*, s63–s74. https://doi.org/10.1017/S1751731118000319

Hashimoto, S., Minami, N., Yamada, M., & Imai, H. (2000). Excessive concentration of glucose during in vitro maturation impairs the developmental competence of bovine oocytes after in vitro fertilization: Relevance to intracellular reactive oxygen species and glutathione contents. *Molecular Reproduction and Development*, *56*(4), 520–526. https://doi.org/10.1002/1098-2795(200008)56:4<520::AID-MRD10>3.0.CO;2-0

Hentze, M. W., Castello, A., Schwarzl, T., & Preiss, T. (2018). A brave new world of RNA-binding proteins. *Nature Reviews Molecular Cell Biology*, *19*(5), 327–341. https://doi.org/10.1038/nrm.2017.130

Kennedy, C. E., Krieger, K. B., Sutovsky, M., Xu, W., Vargovič, P., Didion, B. A., Ellersieck, M. R., Hennessy, M. E., Verstegen, J., Oko, R., & Sutovsky, P. (2014). Protein expression pattern of PAWP in bull spermatozoa is associated with sperm quality and fertility following artificial insemination: PROTEIN EXPRESSION PATTERN OF PAWP. *Molecular Reproduction and Development*, *81*(5), 436–449. https://doi.org/10.1002/mrd.22309

Kerns, K., Zigo, M., Drobnis, E. Z., Sutovsky, M., & Sutovsky, P. (2018). Zinc ion flux during mammalian sperm capacitation. *Nature Communications*, *9*(1), 2061. https://doi.org/10.1038/s41467-018-04523-y

Kopito, R. R. (2000). Aggresomes, inclusion bodies and protein aggregation. *Trends in Cell Biology*, *10*(12), 524–530. https://doi.org/10.1016/S0962-8924(00)01852-3

Krisher, R. L. (2003). *The effect of oocyte quality on development*. 10.

Kuhn, M. T., Hutchison, J. L., & Norman, H. D. (2008). Modeling Nuisance Variables for Prediction of Service Sire Fertility. *Journal of Dairy Science*, *91*(7), 2823–2835. https://doi.org/10.3168/jds.2007-0946

Kuznetsov, A. V., Kehrer, I., Kozlov, A. V., Haller, M., Redl, H., Hermann, M., Grimm, M., & Troppmair, J. (2011). Mitochondrial ROS production under cellular stress: Comparison of different detection methods. *Analytical and Bioanalytical Chemistry*, *400*(8), 2383–2390. https://doi.org/10.1007/s00216-011-4764-2

Madan, P., Rose, K., & Watson, A. J. (2007). Na/K-ATPase β1 Subunit Expression Is Required for Blastocyst Formation and Normal Assembly of Trophectoderm Tight Junction-associated Proteins. *Journal of Biological Chemistry*, *282*(16), 12127–12134. https://doi.org/10.1074/jbc.M700696200

Maurer, R. R., & Chenault, J. R. (1983). Fertilization Failure and Embryonic Mortality in Parous and Nonparous Beef Cattle1. *Journal of Animal Science*, *56*(5), 1186–1189. https://doi.org/10.2527/jas1983.5651186x

Maxwell, W., Parrilla, I., Caballero, I., Garcia, E., Roca, J., Martinez, E., Vazquez, J., & Rath, D. (2007). Retained Functional Integrity of Bull Spermatozoa after Double Freezing and Thawing Using PureSperm® Density Gradient Centrifugation: Double Freezing of Bull Spermatozoa. *Reproduction in Domestic Animals*, *42*(5), 489–494. https://doi.org/10.1111/j.1439-0531.2006.00811.x

Mayran, A., & Drouin, J. (2018). Pioneer transcription factors shape the epigenetic landscape. *Journal of Biological Chemistry, 293*(36), 13795–13804. https://doi.org/10.1074/jbc.R117.001232

Mayran, A., Khetchoumian, K., Hariri, F., Pastinen, T., Gauthier, Y., Balsalobre, A., & Drouin, J. (2018). Pioneer factor Pax7 deploys a stable enhancer repertoire for specification of cell fate. *Nature Genetics, 50*(2), 259–269. https://doi.org/10.1038/s41588-017-0035-2

Memili, E., & First, N. L. (1999). Control of Gene Expression at the Onset of Bovine Embryonic Development1. *Biology of Reproduction, 61*(5), 1198–1207. https://doi.org/10.1095/biolreprod61.5.1198

Michalak, M., & Gye, M. C. (2015). Endoplasmic reticulum stress in periimplantation embryos. *Clinical and Experimental Reproductive Medicine, 42*(1), 1. https://doi.org/10.5653/cerm.2015.42.1.1

Miyoshi, N., Barton, S. C., Kaneda, M., Hajkova, P., & Surani, M. A. (2006). The continuing quest to comprehend genomic imprinting. *Cytogenetic and Genome Research*, *113*(1–4), 6–11. https://doi.org/10.1159/000090808

Mizushima, N. (2007). Autophagy: Process and function. *Genes & Development, 21*(22), 2861–2873. https://doi.org/10.1101/gad.1599207

Morado, S., Cetica, P., Beconi, M., Thompson, J. G., & Dalvit, G. (2013). Reactive oxygen species production and redox state in parthenogenetic and sperm-mediated bovine oocyte activation. *Reproduction, 145*(5), 471–478. https://doi.org/10.1530/REP-13-0017

Morrell, J., Johannisson, A., Dalin, A.-M., & Rodriguez-Martinez, H. (2009). Morphology and Chromatin Integrity of Stallion Spermatozoa Prepared by Density Gradient and Single Layer Centrifugation Through Silica Colloids. *Reproduction in Domestic Animals*, *44*(3), 512–517. https://doi.org/10.1111/j.1439-0531.2008.01265.x

Mtango, N. R., Sutovsky, M., VandeVoort, C. A., Latham, K. E., & Sutovsky, P. (2012). Essential role of ubiquitin C-terminal hydrolases UCHL1 and UCHL3 in mammalian oocyte maturation. *Journal of Cellular Physiology*, *227*(5), 2022–2029. https://doi.org/10.1002/jcp.22931

Nasr-Esfahani, M. M., & Johnson, M. H. (1991). *The origin of reactive oxygen species in mouse embryos cultured in vitro*. 10.

Naz, R. K., & Rajesh, P. B. (2004). Role of tyrosine phosphorylation in sperm capacitation/acrosome reaction. *Reproductive Biology and Endocrinology*, *2*(1), 75. https://doi.org/10.1186/1477-7827-2-75

Nikas, G., Ao, A., Winston, R. M. L., & Handyside, A. H. (1996). Compaction and Surface Polarity in the Human Embryo in Vitro. *Biology of Reproduction*, *55*(1), 32–37. https://doi.org/10.1095/biolreprod55.1.32

Nishioka, N., Inoue, K., Adachi, K., Kiyonari, H., Ota, M., Ralston, A., Yabuta, N., Hirahara, S., Stephenson, R. O., Ogonuki, N., Makita, R., Kurihara, H., Morin-Kensicki, E. M., Nojima, H., Rossant, J., Nakao, K., Niwa, H., & Sasaki, H. (n.d.). The Hippo Signaling Pathway Components Lats and Yap Pattern Tead4 Activity to Distinguish Mouse Trophectoderm from Inner Cell Mass. *Developmental Cell*, 13.

Nomikos, M., Yu, Y., Elgmati, K., Theodoridou, M., Campbell, K., Vassilakopoulou, V., Zikos, C., Livaniou, E., Amso, N., Nounesis, G., Swann, K., & Lai, F. A. (2013). Phospholipase Cζ rescues failed oocyte activation in a prototype of male factor infertility. *Fertility and Sterility*, *99*(1), 76–85. https://doi.org/10.1016/j.fertnstert.2012.08.035

Norman, H. D., Hutchison, J. L., & VanRaden, P. M. (2011). Evaluations for service-sire conception rate for heifer and cow inseminations with conventional and sexed semen. *Journal of Dairy Science*, *94*(12), 6135–6142. https://doi.org/10.3168/jds.2010-3875

Ortega, M. S., Kelleher, A. M., O'Neil, E., Benne, J., Cecil, R., & Spencer, T. E. (2020). *NANOG* is required to form the epiblast and maintain pluripotency in the bovine embryo. *Molecular Reproduction and Development*, *87*(1), 152–160. https://doi.org/10.1002/mrd.23304

Ortega, M. S., Kurian, J. J., McKenna, R., & Hansen, P. J. (2017). Characteristics of candidate genes associated with embryonic development in the cow: Evidence for a role for WBP1 in development to the blastocyst stage. *PLOS ONE*, *12*(5), e0178041. https://doi.org/10.1371/journal.pone.0178041

Ortega, M. S., Moraes, J. G. N., Patterson, D. J., Smith, M. F., Behura, S. K., Poock, S., & Spencer, T. E. (2018). Influences of sire conception rate on pregnancy establishment in dairy cattle. *Biology of Reproduction*, *99*(6), 1244–1254. https://doi.org/10.1093/biolre/ioy141

Pan, B., & Li, J. (2019). The art of oocyte meiotic arrest regulation. *Reproductive Biology and Endocrinology*, *17*(1), 8. https://doi.org/10.1186/s12958-018-0445-8

Perticarari, S., Ricci, G., Granzotto, M., Boscolo, R., Pozzobon, C., Guarnieri, S., Sartore, A., & Presani, G. (2007). A new multiparameter flow cytometric method for human semen analysis. *Human Reproduction*, *22*(2), 485–494. https://doi.org/10.1093/humrep/del415

Pfeffer, P. L. (2018). Building Principles for Constructing a Mammalian Blastocyst Embryo. *Biology*, *7*(3), 41. https://doi.org/10.3390/biology7030041

Phillips, T. C., Dhaliwal, G. K., Verstegen-Onclin, K. M., & Verstegen, J. P. (2012). Efficacy of four density gradient separation media to remove erythrocytes and nonviable sperm from canine semen. *Theriogenology*, *77*(1), 39–45. https://doi.org/10.1016/j.theriogenology.2011.07.012

Rajabi-Toustani, R., Akter, Q. S., & Almadaly, E. A. (2018). *Methodological Improvement of FITC-PNA Staining*. 28.

Ravanan, P., Srikumar, I. F., & Talwar, P. (2017). Autophagy: The spotlight for cellular stress responses. *Life Sciences*, *188*, 53–67. https://doi.org/10.1016/j.lfs.2017.08.029

Saacke, R. G. (2008). Sperm morphology: Its relevance to compensable and uncompensable traits in semen. *Theriogenology*, *70*(3), 473–478. https://doi.org/10.1016/j.theriogenology.2008.04.012

Sakatani, M. (2017). Effects of heat stress on bovine preimplantation embryos produced *in vitro*. *Journal of Reproduction and Development*, *63*(4), 347–352. https://doi.org/10.1262/jrd.2017-045

Sato, M., & Sato, K. (2013). Maternal inheritance of mitochondrial DNA by diverse mechanisms to eliminate paternal mitochondrial DNA. *Biochimica et Biophysica*

Acta (BBA) - Molecular Cell Research, *1833*(8), 1979–1984. https://doi.org/10.1016/j.bbamcr.2013.03.010

Schatten, H., & Sun, Q.-Y. (2009). The role of centrosomes in mammalian fertilization and its significance for ICSI. *Molecular Human Reproduction*, *15*(9), 531–538. https://doi.org/10.1093/molehr/gap049

Senger, P. (2003). *Pathways to Pregnancy and Parturition* (2nd ed.).

Sies, H., & Chance, B. (1970). The steady state level of catalase compound I in isolated hemoglobin-free perfused rat liver. *FEBS Letters*, *11*(3), 172–176. https://doi.org/10.1016/0014-5793(70)80521-X

Sies, H., & Jones, D. P. (2020). Reactive oxygen species (ROS) as pleiotropic physiological signalling agents. *Nature Reviews Molecular Cell Biology*, *21*(7), 363–383. https://doi.org/10.1038/s41580-020-0230-3

Song, B.-S., Yoon, S.-B., Kim, J.-S., Sim, B.-W., Kim, Y.-H., Cha, J.-J., Choi, S.-A., Min, H.-K., Lee, Y., Huh, J.-W., Lee, S.-R., Kim, S.-H., Koo, D.-B., Choo, Y.-K., Kim, H. M., Kim, S.-U., & Chang, K.-T. (2012). Induction of Autophagy Promotes Preattachment Development of Bovine Embryos by Reducing Endoplasmic Reticulum Stress1. *Biology of Reproduction*, *87*(1). https://doi.org/10.1095/biolreprod.111.097949

Song, W.-H., Yi, Y.-J., Sutovsky, M., Meyers, S., & Sutovsky, P. (2016). Autophagy and ubiquitin–proteasome system contribute to sperm mitophagy after mammalian fertilization. *Proceedings of the National Academy of Sciences*, *113*(36). https://doi.org/10.1073/pnas.1605844113

Stewart, J. B., & Chinnery, P. F. (2015). The dynamics of mitochondrial DNA heteroplasmy: Implications for human health and disease. *Nature Reviews Genetics*, *16*(9), 530–542. https://doi.org/10.1038/nrg3966

Stitzel, M. L., & Seydoux, G. (2007). Regulation of the Oocyte-to-Zygote Transition. *Science*, *316*(5823), 407–408. https://doi.org/10.1126/science.1138236

Susor, A., Liskova, L., Toralova, T., Pavlok, A., Pivonkova, K., Karabinova, P., Lopatarova, M., Sutovsky, P., & Kubelka, M. (2010). Role of Ubiquitin C-Terminal Hydrolase-L1 in Antipolyspermy Defense of Mammalian Oocytes1. *Biology of Reproduction*, *82*(6), 1151–1161. https://doi.org/10.1095/biolreprod.109.081547

Sutovsky, P. (2018). Review: Sperm–oocyte interactions and their implications for bull fertility, with emphasis on the ubiquitin–proteasome system. *Animal*, *12*, s121–s132. https://doi.org/10.1017/S1751731118000253

Sutovsky, P., Aarabi, M., Miranda-Vizuete, A., & Oko, R. (2015). Negative biomarker based male fertility evaluation: Sperm phenotypes associated with molecular-level anomalies. *Asian Journal of Andrology*, *17*(4), 554. https://doi.org/10.4103/1008-682X.153847

Sutovsky, P., Moreno, R. D., Ramalho-Santos, J., Dominko, T., Simerly, C., & Schatten, G. (1999). Ubiquitin tag for sperm mitochondria. *Nature*, *402*(6760), 371–372. https://doi.org/10.1038/46466

Sutovsky, P., Moreno, R. D., Ramalho-Santos, J., Dominko, T., Simerly, C., & Schatten, G. (2000). Ubiquitinated Sperm Mitochondria, Selective Proteolysis, and the

Regulation of Mitochondrial Inheritance in Mammalian Embryos1. *Biology of Reproduction*, *63*(2), 582–590. https://doi.org/10.1095/biolreprod63.2.582

Sutovsky, P., Navara, C. S., & Schatten, G. (1996). Fate of the Sperm Mitochondria, and the Incorporation, Conversion, and Disassembly of the Sperm Tail Structures during Bovine Fertilization1. *Biology of Reproduction*, *55*(6), 1195–1205. https://doi.org/10.1095/biolreprod55.6.1195

Sutovsky, P., Neuber, E., & Schatten, G. (2002). Ubiquitin-dependent sperm quality control mechanism recognizes spermatozoa with DNA defects as revealed by dual ubiquitin-TUNEL assay. *Molecular Reproduction and Development*, *61*(3), 406–413. https://doi.org/10.1002/mrd.10101

Tomlinson, M. J., Moffatt, O., Manicardi, G. C., Bizzaro, D., Afnan, M., & Sakkas, D. (2001). Interrelationships between seminal parameters and sperm nuclear DNA damage before and after density gradient centrifugation: Implications for assisted conception. *Human Reproduction*, *16*(10), 2160–2165. https://doi.org/10.1093/humrep/16.10.2160

Tsukamoto, S., Kuma, A., & Mizushima, N. (2008). The role of autophagy during the oocyte-to-embryo transition. *Autophagy*, *4*(8), 1076–1078. https://doi.org/10.4161/auto.7065

van Soom, A., Ysebaert, M.-T., & de Kruif, A. (1997). Relationship between timing of development, morula morphology, and cell allocation to inner cell mass and trophectoderm in in vitro-produced bovine embryos. *Molecular Reproduction and Development*, *47*(1), 47–56. https://doi.org/10.1002/(SICI)1098-2795(199705)47:1<47::AID-MRD7>3.0.CO;2-Q

Violette, M. I., Madan, P., & Watson, A. J. (2006). Na+/K+-ATPase regulates tight junction formation and function during mouse preimplantation development. *Developmental Biology*, *289*(2), 406–419. https://doi.org/10.1016/j.ydbio.2005.11.004

Wang, H., & Dey, S. K. (2006). Roadmap to embryo implantation: Clues from mouse models. *Nature Reviews Genetics*, *7*(3), 185–199. https://doi.org/10.1038/nrg1808

Wang, M., Wey, S., Zhang, Y., Ye, R., & Lee, A. S. (2009). Role of the Unfolded Protein Response Regulator GRP78/BiP in Development, Cancer, and Neurological Disorders. *Antioxidants & Redox Signaling*, *11*(9), 2307–2316. https://doi.org/10.1089/ars.2009.2485

Wiltbank, M. C., Baez, G. M., Garcia-Guerra, A., Toledo, M. Z., Monteiro, P. L. J., Melo, L. F., Ochoa, J. C., Santos, J. E. P., & Sartori, R. (2016). Pivotal periods for pregnancy loss during the first trimester of gestation in lactating dairy cows. *Theriogenology*, *86*(1), 239–253. https://doi.org/10.1016/j.theriogenology.2016.04.037

Wong, E. S. P., Tan, J. M. M., Soong, W.-E., Hussein, K., Nukina, N., Dawson, V. L., Dawson, T. M., Cuervo, A. M., & Lim, K.-L. (2008). Autophagy-mediated clearance of aggresomes is not a universal phenomenon. *Human Molecular Genetics*, *17*(16), 2570–2582. https://doi.org/10.1093/hmg/ddn157

Wu, A. T. H., Sutovsky, P., Manandhar, G., Xu, W., Katayama, M., Day, B. N., Park, K.-W., Yi, Y.-J., Xi, Y. W., Prather, R. S., & Oko, R. (2007). PAWP, a Sperm-specific WW Domain-binding Protein, Promotes Meiotic Resumption and

Pronuclear Development during Fertilization. *Journal of Biological Chemistry*, *282*(16), 12164–12175. https://doi.org/10.1074/jbc.M609132200

Yamamoto, A., Mizushima, N., & Tsukamoto, S. (2014). Fertilization-Induced Autophagy in Mouse Embryos is Independent of mTORC11. *Biology of Reproduction*, *91*(1). https://doi.org/10.1095/biolreprod.113.115816

Yang, H. W., Hwang, K. J., Kwon, H. C., Kim, H. S., Choi, K. W., & Oh, K. S. (1998). Detection of reactive oxygen species (ROS) and apoptosis in human fragmented embryos. *Human Reproduction*, *13*(4), 998–1002. https://doi.org/10.1093/humrep/13.4.998

Yoon, S.-B., Choi, S.-A., Sim, B.-W., Kim, J.-S., Mun, S.-E., Jeong, P.-S., Yang, H.-J., Lee, Y., Park, Y.-H., Song, B.-S., Kim, Y.-H., Jeong, K.-J., Huh, J.-W., Lee, S.-R., Kim, S.-U., & Chang, K.-T. (2014). Developmental Competence of Bovine Early Embryos Depends on the Coupled Response Between Oxidative and Endoplasmic Reticulum Stress1. *Biology of Reproduction*, *90*(5). https://doi.org/10.1095/biolreprod.113.113480

Yu, Y., Xu, W., Yi, Y.-J., Sutovsky, P., & Oko, R. (2006). The extracellular protein coat of the inner acrosomal membrane is involved in zona pellucida binding and penetration during fertilization: Characterization of its most prominent polypeptide (IAM38). *Developmental Biology*, *290*(1), 32–43. https://doi.org/10.1016/j.ydbio.2005.11.003

Zeeshan, H., Lee, G., Kim, H.-R., & Chae, H.-J. (2016). Endoplasmic Reticulum Stress and Associated ROS. *International Journal of Molecular Sciences*, *17*(3), 327. https://doi.org/10.3390/ijms17030327

Zernicka-Goetz, M., Morris, S. A., & Bruce, A. W. (2009). Making a firm decision: Multifaceted regulation of cell fate in the early mouse embryo. *Nature Reviews Genetics, 10*(7), 467–477. https://doi.org/10.1038/nrg2564

Zuidema, D., Kerns, K., & Sutovsky, P. (2021). An Exploration of Current and Perspective Semen Analysis and Sperm Selection for Livestock Artificial Insemination. *Animals, 11*(12), 3563. https://doi.org/10.3390/ani11123563

Zuidema, D., & Sutovsky, P. (2020). The domestic pig as a model for the study of mitochondrial inheritance. *Cell and Tissue Research, 380*(2), 263–271. https://doi.org/10.1007/s00441-019-03100-z